STUDY OF LAMINAR FLOW FORCED CONVECTION HEAT TRANSFER BEHAVIOR OF A PHASE CHANGE MATERIAL FLUID

A Thesis

by

GURUNARAYANA RAVI

Submitted to the Office of Graduate Studies of
Texas A&M University
in partial fulfillment of the requirements for the degree of

MASTER OF SCIENCE

December 2008

Major Subject: Mechanical Engineering

STUDY OF LAMINAR FLOW FORCED CONVECTION HEAT TRANSFER BEHAVIOR OF A PHASE CHANGE MATERIAL FLUID

A Thesis

by

GURUNARAYANA RAVI

Submitted to the Office of Graduate Studies of
Texas A&M University
in partial fulfillment of the requirements for the degree of

MASTER OF SCIENCE

Approved by:

Co-Chairs of Committee,	Jorge Alvarado
	Sai Lau
Committee Members,	Othon Rediniotis
Head of Department,	Dennis O' Neal

December 2008

Major Subject: Mechanical Engineering

ABSTRACT

Study of Laminar Flow Forced Convection Heat Transfer Behavior of a

Phase Change Material Fluid. (December 2008)

Gurunarayana Ravi, B.E., Anna University, India

Co-Chairs of Advisory Committee: Dr. Jorge Alvarado
Dr. Sai Lau

The heat transfer behavior of phase change material fluid under laminar flow conditions in circular tubes and internally longitudinal finned tubes are presented in this study. Two types of boundary conditions, including uniform axial heat flux with constant peripheral temperature and uniform axial and peripheral temperature, were considered in the case of circular tubes. An effective specific heat technique was used to model the phase change process assuming a hydrodynamically fully-developed flow at the entrance of the tube. Results were also obtained for the phase change process under hydro dynamically and thermally fully developed conditions. In case of a smooth circular tube with phase change material (PCM) fluid, results of Nusselt number were obtained by varying the bulk Stefan number. The Nusselt number results were found to be strongly dependent on the Stefan number. In the case of a finned tube two types of boundary conditions were studied. The first boundary condition had a uniform axial heat flux along the axis of the tube with a variable temperature on the peripheral surface of the tube. The second boundary condition had a constant temperature on the outer surface of the tube. The effective specific heat technique was again implemented to analyze the

phase change process under both the boundary conditions. The Nusselt number was determined for a tube with two fins with different fin height ratios and fin thermal conductivity values. It was determined that the Nusselt number was strongly dependent on the Stefan number, fin thermal conductivity value, and height of the fins. It was also observed that for a constant heat axial flux boundary condition with peripherally varying temperature, the phase change slurry with the internally finned tube performed better than the one without fins. A similar trend was observed during the phase change process with internal fins under the constant wall temperature boundary condition.

DEDICATION

To my family and friends for their love, support and understanding.

ACKNOWLEDGEMENTS

I would like to express my sincere gratitude to several people who made this thesis possible. First of all, I would like to thank my co-chair and advisor, Dr. Jorge Alvarado, for giving his time and sharing his knowledge on the subject with me. He has always been keen to help me out throughout the course of this research. I would like to thank my other co-chair, Dr. Sai Lau, and my committee member, Dr. Othon Rediniotis, for their valuable input.

Additionally, I want to thank Dr. David Kessler from Laboratory for Computational Physics and Fluid Dynamics, Naval Research Laboratory for his kind support in sharing his knowledge and help with writing user defined functions for FLUENT.

In closing, I want to thank my parents, Mr. Ravi Srinivasan and Mrs. Mythili Ravi, friends, and my other family members for encouraging me to pursue higher education. My parents, friends, and family members have been the pillars of support in difficult times and always believed in my capabilities.

NOMENCLATURE

Variables

a	Local radial co-ordinate
A_r	Aspect ratio
c	Volumetric concentration
c_m	Mass concentration
Cp	Specific heat
D	Diameter of the tube
e	Velocity gradient
f	Constant
g	Enthalpy
H	Fin height ratio
h (z)	Heat transfer coefficient at a distance z from the inlet
k	Thermal conductivity
K	Fin conductance ratio
l	Tube length
L	Latent heat
$\dot{m}$	Mass flow rate of the slurry or fluid
M	Number of fins
Nu	Nusselt number
P	Perimeter of the tube
Pr	Prandtl Number

q	Heat
Q	Total heat transfer rate at solid-fluid interface
r	Radius of the tube
Ste	Stefan number
t	Fin height
T	Temperature
T (z)	Temperature at a distance z from the inlet
u	Velocity in x direction
v	Velocity in y direction
w	Velocity in z direction
x	Cartesian co-ordinate along x direction
y	Cartesian co-ordinate along y direction
z	Cartesian co-ordinate along z direction

Greek symbols

a	Thermal diffusivity
ζ	Dimensionless length
θ	Dimensionless temperature
μ	Dynamic viscosity
ν	Kinematic viscosity
ρ	Density
ψ	Half the fin angle

Subscripts

Al	Aluminum
avg	Average
b	Bulk
d	Based on tube diameter
e	Effective
f	Water
H	Constant wall heat flux
i	Inlet
j	Local value
k	Local value
lm	Log mean value
m	Melting point
mean	Mean
o	Outlet
p	Phase change particle
s	Fin
sl	Slurry
T	Constant wall temperature
u	Unfinned surface
w	Wall
1	Start of melting
2	End of melting

Superscripts

``	Flux
-	Average

Acronyms

BC	Boundary Condition
CHF	Constant Heat Flux
CWT	Constant Wall Temperature
MPCM	Micro Encapsulated Phase Change Material
PCM	Phase Change Material

TABLE OF CONTENTS

Page

Page

LIST OF FIGURES

Page

Page

Page

1. INTRODUCTION

1.1 Internally finned tubes

Internally finned tubes have acquired importance over the years in a variety of heat transfer applications including compact heat exchangers. Fins increase the effective heat transfer area and convective heat transfer thus improving the performance of the heat exchanger. Various configurations of internally finned tubes like longitudinal, helical, annular have been studied both experimentally and numerically, and have demonstrated enhancement in heat transfer. Various cross sections of fins like triangular and trapezoidal have also been studied and their performances have been validated numerically. From the investigations for a longitudinal fin of a trapezoidal cross section, the parameters influencing the performance of the heat exchanger were found to be the thermal conductivity of the fin, height of the fin, and number of fins.

1.2 Phase change materials

Phase change materials (PCM) have significant latent heat capacity and thus provide an excellent means of storing thermal energy. One of the main required properties of PCM is that it should have high storage density. Other preferable properties of PCM include low volume change during the phase change process, cycling stability,

---

This thesis follows the style of International Journal of Heat and Mass Transfer.

and high apparent specific heat. Some examples of PCM's are paraffin and salt hydrates. Paraffins are organic PCMs which are thermally stable and non corrosive. Salt hydrates are corrosive and have very poor cycling capability though they have a high melting enthalpy per unit volume.

1.3 Motivation for current work

Internal longitudinal fins in circular tubes are widely used in high performance compact heat exchangers with major applications in aerospace, petroleum, automotive and chemical industries. Phase change materials are also being used as alternative cooling methods in thermal management of electronics and energy storage module for space-based activities. These PCM slurries due to their thermal capacity enhance the overall thermal performance of heat transfer systems. Though phase change materials have a high energy storage density, the major drawback is low thermal conductivity of phase change materials that are currently available. Thus it is necessary to study alternate ways to improve the performance of PCM-based heat exchangers.

With a thorough literature survey in the area of enhanced heat transfer and phase change materials, it was found that both numerical and experimental data was lacking specifically in the area of heat transfer of PCM-based slurry in internally finned tubes. With internally finned tubes being widely used in compact heat exchangers and PCM-based fluids gaining popularity in fields of heating, ventilation and air-conditioning, it was decided to study numerically the effects of phase change material flowing inside a finned tube.

1.4 Significance of current work

Numerous studies on heat transfer enhancement have been studied by using single phase fluids, phase change materials, phase change material slurries, dispersed highly conductive particles among many. But relatively very few studies have been performed to study the effects of a phase change materials with enhanced surfaces. These studies are needed as there are limited number of useable heat transfer fluids and practical enhanced surface configurations that are available for commercial use.

This study has investigated the performance of a circular tube heat exchanger with longitudinal internal fins with phase change material slurry. It has also taken advantage of prior experimental and numerical work done on single phase fluids with longitudinal internal fins in a circular tube. It has also considered previous experimental and numerical work done with phase change materials in a circular tube. Since the combined effect of phase change material and the use of an internally finned tube have not been fully investigated experimentally or computationally, a computational fluid dynamics approach has been used to investigate the heat transfer behavior of phase change material fluids in smooth and internally-finned tubes.

A realistic fin configuration has been studied where the tip of the fin is a circular arc concentric with the tube. Also finite thermal conductivity value (as of Aluminum) for the fin was considered during the study in combination with the phase change material slurry. Usually finned tube studies have assumed a constant axial heat flux with a peripherally uniform temperature as the boundary condition. Here a type of boundary condition called the H2 boundary condition [1] was used in the case of constant wall

heat flux boundary condition in an internally finned tube. The finned tube had a constant axial heat flux with a constant peripheral heat flux (which also implies the peripheral wall temperature is variable). This is the true boundary condition experienced by a carrier fluid like water when it flows in a finned tube of high thermal conductivity such as aluminum. Thus this study depicted the heat transfer performance closer to the exact phenomenon that happens in heat exchangers.

1.5 Aim and objectives of current study

As a first step, a smooth circular pipe was modeled using a CFD software package to numerically test and validate the well-established closed-form values of internal laminar flow with constant heat flux or constant wall temperature without phase change material suspensions. Then the study extended to validate the performance of phase change slurry in a smooth tube with and without the enhanced thermal conductivity model [2].

Then evaluation of the performance of an internally finned tube with the phase change material slurry was undertaken. Two different boundary conditions were evaluated. One was the constant wall heat flux condition with axially and peripherally uniform heat flux, while the other being a constant wall temperature condition. In case of the internally finned tube with fins located diametrically opposite to each other, two fin thermal conductivities (one equal to the bulk thermal conductivity of the PCM fluid and one equal to aluminum) were used along with three different fin heights. Several values of Stefan number were used for constant wall heat flux case with the H2

boundary condition, and constant wall temperature boundary condition. As a part of the study, the effect of phase change material melting under thermally and hydrodynamically fully developed condition was also considered.

2. LITERATURE REVIEW

In this section, a brief background of internally finned tubes and phase change materials are presented. The section has been divided into two parts. The first section focuses on the modeling aspects of internally finned tubes for constant wall heat flux and constant wall temperature boundary conditions. The second section focuses on the theory and modeling aspects of phase change materials in a smooth circular tube.

2.1 Modeling of heat transfer in internally finned tubes

Numerous studies have been done on the thermal performance of internal longitudinal fins in a circular tube. A two dimensional internally finned tube was studied using constant heat flux (H) and constant temperature (T) boundary condition under hydrodynamically fully developed flow and thermally developing flow conditions [3]. It was found that for very small values of dimensionless axial distance, the rate of decrease of the local Nusselt number was found to be same as that of a smooth tube, but sharp temperature gradients were observed in the developing region. This behavior was attributed to the fin height (t), fin angle (2 ψ), ratio of solid-to-fluid thermal conductivity (also called fin conductance ratio (K)) of the finned tube.

Results were obtained for the entrance region of an internally finned tube with zero fin thickness (extremely thin) and infinite (very high) thermal conductivity [4]. A fin of zero thickness is understood as a straight longitudinal fin with a negligible thickness in the angular direction. Two boundary conditions namely T1 [1] and H1 [1]

boundary condition were numerically validated. Results and values for Nusselt number within the hydrodynamic thermally developed lengths were presented based on the outer diameter and the equivalent hydraulic diameter of a circular duct. The results exhibited large pressure gradients in the entrance region.

For a finite fin thermal conductivity, and taking into account the three dimensional nature of the fin [5], it was found that the ratio of solid-to-fluid thermal conductivity (K) affects the overall heat transfer process. There is also a significant over estimation in the resulting Nusselt number by assuming the wall temperature to be the same as the fin temperature for small values of K. This is because the assumption holds true only for an infinite value of K. Also this means that there is no temperature distribution inside and on the surface of the fin which is not true for a fin of finite thermal conductivity. Results of an internally finned tube with different fin heights and uniform wall temperature [6] reported an increase in coefficient of friction when the fin height and the number of fins were increased. An eight-fold increase in Nusselt number as compared with a smooth circular pipe could be achieved when 4-8 fins were used with a fin height ratio (ratio of the height of the fin to the radius of the tube) of 0.6. The fin height ratio equation is given in Eq. (1).

$$H = \frac{t}{r} \tag{1}$$

Where H, t, and r are the height ratio, fin height and the radius of the tube respectively. Each variable is depicted in Fig. 1.

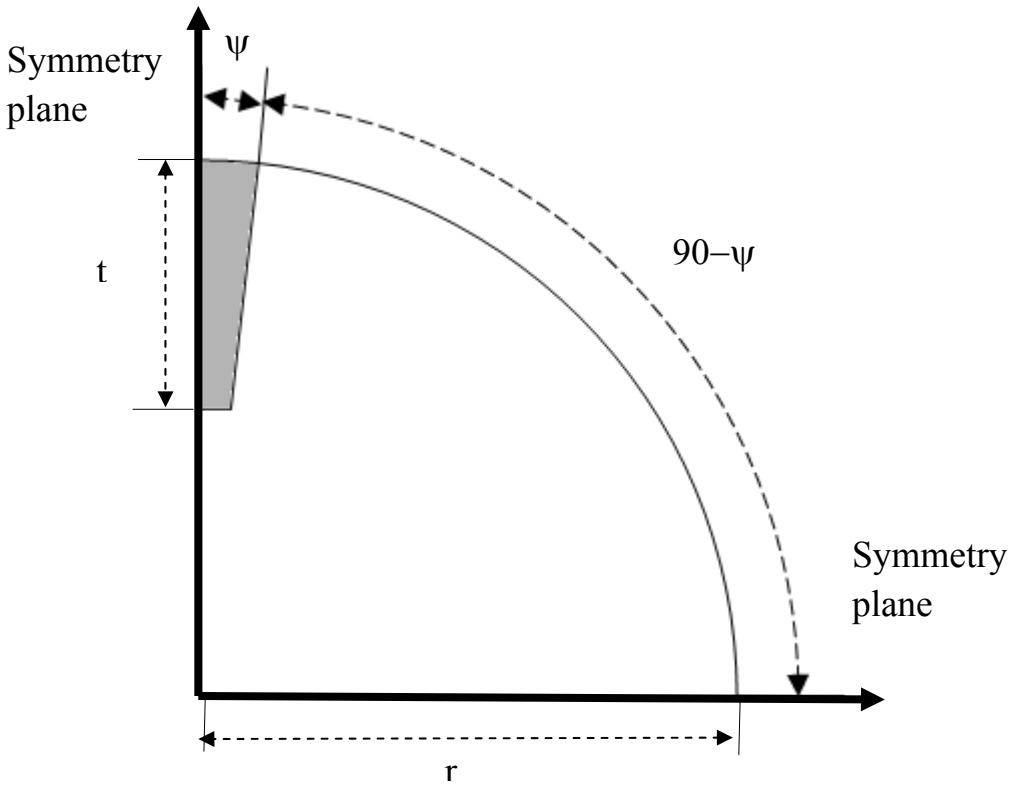

Fig. 1. Internal fins in a smooth circular tube.

Studies focusing on optimizing finned tube performance have already been under taken by other investigators [7, 8]. It has been observed that small numbers of long fins can double the heat exchanger performance while keeping pumping power low [7]. Furthermore, an optimum number of fins are desirable for a particular fin configuration [8]. This study was based on a numerical simulation of a triangular internally finned tube with 100 percent fin effectiveness and a hydrodynamically and thermally fully flow. Fin effectiveness is defined as the ratio between the local heat flux on the side of the fins, and the average heat flux at the solid-fluid interface excluding the tip of the fin surface as shown in Eq. (2).

$$\text{Effectiveness} = \frac{q_u}{\left(Q/2M\left(\psi r + t\right)\right)} \qquad (2)$$

Where, q_u, Q, M,ψ, t are heat flux on the un-finned surface, heat transfer rate, number of fins, half the fin angle and fin height respectively. Various analytical studies including forced convective heat transfer with laminar flow have been performed on longitudinal internal finned tubes. The effect of thermal conductivity of the fin on heat transfer for an internally finned tube was also studied analytically [9]. The heat transfer characteristics were found to be dependent on the fin configuration and fin conductivity. The magnitude of the effect of fin conductivity on temperature and Nusselt number was significant for fin height ratio greater than 0.4. A longitudinal internally finned tube of a trapezoidal cross section was studied by dividing the flow domain into two regions [10]. It was found that the dimensionless velocity was dependent on the number of fins, fin height and the fin angle (angle between the flanks of two adjacent fins). For a given number of fins, secondary velocity loops could be seen only after a critical value of fin height ratio. It was also found that the formation of a secondary velocity loop depended only on the fin height for a given number of fins. The velocity loop mainly existed for short fins with a large number of fins, and at longer fin heights for smaller number of fins. For example in case of a tube with 4 fins, secondary loops were started to form within $0.4 < H < 0.5$ and for a tube with 28 fins secondary loops were seen for $0.1 < H < 0.2$. An analytical study of the heat transfer characteristics for a laminar flow in a tube with a trapezoidal cross section was studied with constant surface heat flux on the wall surface and a peripherally uniform wall temperature [11]. In this study, for combinations

of fin angle, fin heights and K, Nusselt number was found to increase up to a critical number of fins and later decrease. Laminar heat transfer in a finned tube with a constant wall temperature and a peripherally constant temperature was also studied by Soliman et al. [12]. A similar trend in Nusselt number was observed for various configurations as seen in [11].

2.2 Modeling of heat transfer of phase change material fluids

A number of studies, both experimental and numerical have been performed on phase change materials. A general implicit source-based enthalpy method was proposed for the analysis of a solidification process [13]. Experimental and numerical studies were carried out to characterize the melting of the phase change material in a shell [14]. The problem was modeled in FLUENT 6.3 (CFD software) as a two-phase problem, and it was observed that towards the end of the solidification process irregularities were present along the phase front due to the formation of voids caused by the shrinkage of the PCM. In the same study a numerical method was used to model a moving boundary taking into account freezing and melting a saturated liquid inside a cylindrical or a spherical container with a constant heat transfer coefficient [15]. This analysis used a source-term approach to predict the heat transfer during the melting of the encapsulated phase change material particle.

A comprehensive numerical study on heat transfer of phase change material slurry for constant wall temperature and constant wall heat flux was done by modifying the energy equation to accommodate a heat source term [16], but the model did not take

into account the effects of sub-cooling and specific heat increase in the microcapsules. This work was improved by simulating the melting problem by using a temperature-dependent model instead of a quasi steady model [17]. Here the melting problem in a sub-cooled sphere was solved by considering the crust of the micro capsule. Zhang et al. [17] also studied the heat transfer in microencapsulated phase change slurry flowing through a smooth circular tube. A constant wall temperature problem was solved using the variable specific heat model as used by Roy and Avanic [18]. The results obtained were within 0.3 percent of the results shown in Charunyakorn et al. [16]. Another numerical approach consisted in modelling the melting range numerically using a value of 10^{-4} instead of zero. Various other specific heat functions apart from the rectangular case were used and the solutions were predicted by the specific heat functions which were found to be within five percent of the value predicted by the rectangular case.

Numerical methods were also used to postulate correlations which could predict wall temperature [19]. The effective specific heat method was used to model phase change process, and the accuracy of the specific heat model was comparable with experimental results for Stefan number of 5.4 and a 10% volume concentration of the phase change particles. In another study, a significant increase in heat transfer was reported for an increase in bulk Reynolds number for a given particle concentration, Stefan number, and melting point [20]. Heat transfer enhancement was also found to be higher in the fully developed region than the thermal entry region. Various specific heat functions were investigated and it was determined that the differences in Nusselt number value reported by each function could be neglected for aspect ratios greater than 500

(where aspect ratio is the ratio of the length of the tube to the radius of the tube). This was because all the specific heat functions converged to the same Nusselt number for aspect ratios greater than 500. The aspect ratio is defined in Eq. (3).

$$A_r = \frac{l}{r} \tag{3}$$

Where, Ar and l are the aspect ratio and the tube length respectively. An ice slurry flow in a tube was also studied numerically based on the average properties of the fluid instead of considering them as particles in water [21]. In another study a three region melting model for phase change slurry was proposed [22]. The first region is the sub-cooled region where the particle does not melt and the entire heat is absorbed or rejected only due to the specific heat capacity of the slurry. The second region the particle melts, and heat transfer is due to both latent and specific heat capacity of the slurry (mixture of phase change material and water). The third region is the region where melting is complete and heat transfer takes place while the specific heat of the slurry remains constant. The local heat transfer coefficient in those cases changed in the three melting regions due to the percentage of the particles that melted. An experimental study [23] showed that there is a range of temperature within which a phase change material melts which should be taken into account while performing any CFD simulation. The factors affecting heat transfer were found to be concentration of microcapsules, inlet temperature, duct radius, and ratio of sensible-to-latent heat of the heat transfer fluid.

An experimental study of the heat transfer characteristics of MPCM showed that in the case of laminar flow, the local heat transfer coefficient was higher than for single phase fluids due to latent heat effect during melting, and micro convective thermal

conductivity enhancement [24]. Correlations were developed for determining Nusselt number in the laminar regime. Observations were also made regarding the flow structure of the MPCM slurry laminar case [25].

In a study by Marcel et al. [26], a shell and tube configuration with annular fins between the shell and tube, PCM on the shell side, and the heat transfer fluid circulating in the tube side were analyzed. Marcel et al. [26] numerically and experimentally studied effects of the shell radius, mass flow rate, inlet temperature and annular fins on the heat transfer behavior of the heat exchanger. They found that the annular fins were effective for mass flow rates between 0.0015 kg/s and 0.015kg/s and inlet temperatures of 5K. The PCM used in the study was n-Octadecane.

The background study suggests that virtually no research has been done on internally finned tubes carrying phase change material slurry. The research either corresponds to internally finned tubes with single phase fluid or phase change slurry flowing through a smooth tube with or without external fins.

3. METHODOLOGY

3.1 Formulation of the problem

In this section the governing equations and the assumptions made in modeling the phase change process in an internally finned tube will be discussed.

3.1.1 Governing equations

The modeling of phase change material (PCM) fluid under constant heat flux and temperature was based on the discretization of the continuity, momentum and energy equations as given in equations (4)-(6) respectively.

$$\frac{\partial u_i}{\partial x_i} = 0 \tag{4}$$

$$\frac{\partial}{\partial x_j}(\rho u_i u_j) = -\frac{\partial p}{\partial x_i} + \mu \frac{\partial^2 u_i}{\partial x_k \partial x_k} \tag{5}$$

$$\frac{\partial}{\partial x_i}(u_i\left(\rho\left(g - \frac{p}{\rho} + \frac{u_i u_i}{2}\right)\right) + p)) = \frac{\partial}{\partial x_i}(k_e \frac{\partial T}{\partial x_i}) \tag{6}$$

The above governing equations are solved using the finite volume technique. The equations were discretized and solved numerically using FLUENT 6.3 which is commercial and academic computational fluid dynamic software.

3.1.2 Assumptions

Various assumptions have been made in solving the phase change problem in the past. The phase change slurry is considered to be a Newtonian fluid as long as the maximum volume of the phase change material is less than 25% of the carrier fluid. This assumption simplifies the numerical simulation of PCM fluids as heat transfer fluids since viscosity is assumed to be constant with respect to fluid velocity and temperature. The flow is assumed to be hydrodynamically fully developed and thermally developing laminar flow. This is also true in an internally finned tube with and without phase change material fluid. The phase change materials melt through a range of temperatures, and the slurry inlet temperature is not allowed to be higher than the than the corresponding melting point of the PCM. A three region model has been proposed and implemented, and explained in the earlier section. Other assumptions include temperature-dependent specific heat function, and constant viscosity and density. These assumptions allowed treating PCM fluids as homogeneous liquids. Also, negligible interfacial thermal resistance in the micro capsule and no other heat sources (sink or source) except for the micro capsule are assumed. Values such as for pipe radius (0.001 m or 10 mm), fluid Reynolds number (Re_b = 485) and Grashof number (Gr = 0.001) were used to neglect the natural convection and surface tension effects.

3.2 Source term approach vs. effective specific heat approach

One of the first attempts to numerically model a phase change slurry flow in a circular tube was undertaken by Charunyakorn et al. [16] who used a source term to model the phase change process. The source term represents the amount of heat absorbed or released during the phase change process. This model assumed that natural convection was negligible for very small spheres. It also assumed that the particles entirely consisted of the phase change material and neglected the crust or shell of the microcapsules. The source term is a function of the radius of the phase change particle, localized temperature, thermal conductivity of the particle, concentration of the particle, and the particle Biot number. To obtain the particle radius Charunyakorn et al. [16] solved a fourth order equation as function of r_p (particle radius) which depends on the location in the tube, localized temperature, and Biot number. It was found that using the source term was computationally expensive and complicated. A study by Avanic et al. [19] showed that comparable results could be achieved by using a simpler specific heat approach to model the phase change problem. In their study, it was found that the shape (i.e. triangular, rectangular, or sinusoidal profile) of the specific heat function was not a sensitive parameter in determining the heat performance of MPCM slurry.

Thus it was decided to use the effective heat capacity method to model the convective and phase change process using a computational fluid dynamics software (i.e. FLUENT 6.3). To adopt this method, first the tube is split into three regions as suggested by Choi et al. [22]. Fig. 2 shows the three distinct average temperature regions including sub-cooling, melting, and after melting. According to Choi et al. [21] the location of the

melting process depends on radial distance because of the laminar flow velocity profile as depicted in Fig. 3. This method is also called as the slope-method which is based on the gradient of enthalpy-temperature curve as seen in Fig. 4. The specific heat of the PCM fluid takes into account the specific heat of the carrier fluid in the first and the third regions in the tube, as well as the latent heat capacity and the temperature range of the PCM during the phase change process. A pure substance will have a unique melting temperature whereas a binary mixture can melt through a range of temperatures. In this method all physical and thermal properties of the PCM fluid are calculated based on the volume averaged values of the properties of the particle (an encapsulated phase change material like 1-bromo hexadecane) and the carrier fluid (water).

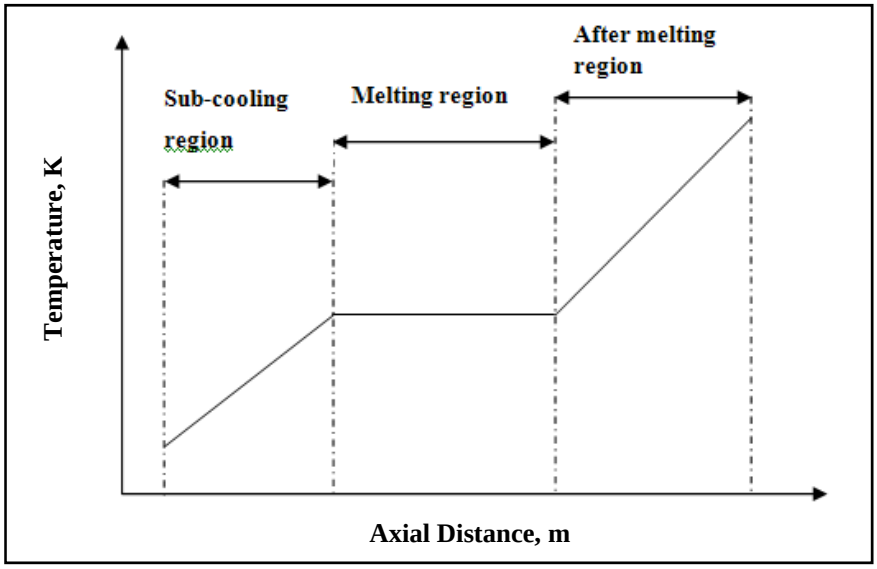

Fig. 2. Average temperature variation with axial distance.

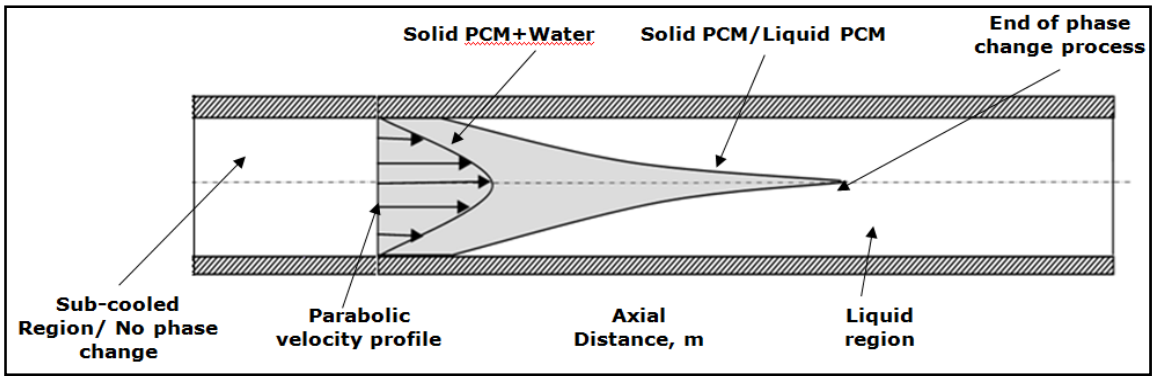

Fig. 3. Melting phenomenon in a circular tube.

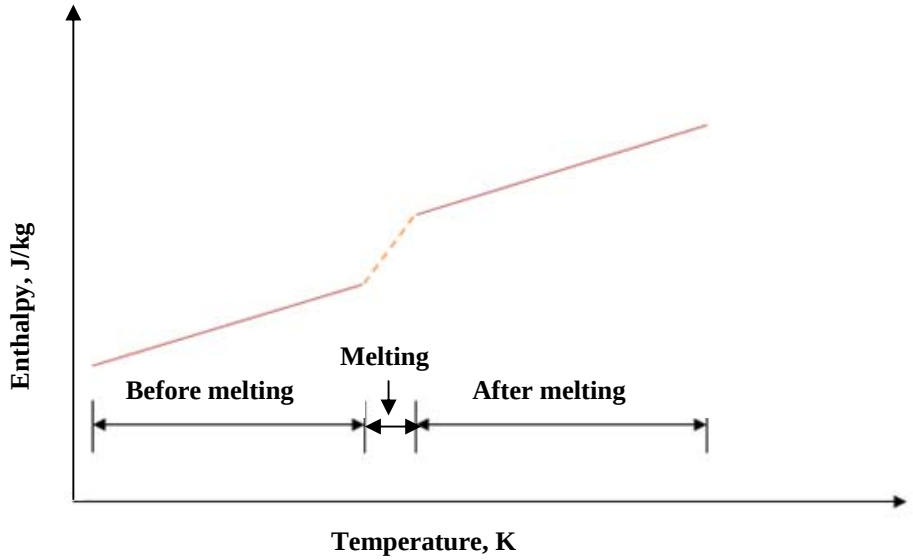

Fig. 4. Variation of specific heat with temperature.

3.3 Boundary conditions

Several thermal boundary conditions were considered in the study. They can be classified as follows:

i. Constant axial wall temperature (T).

ii. Constant axial wall heat flux (H).

iii. A combination of constant axial wall temperature and heat flux.

The possible combinations of boundary conditions for these two cases are specified by adding 1, 2, 3, or 4 to H and T. The numerals indicate a variation in heat flux or temperature for a given H or T boundary condition. In this study, H1 and H2 boundary condition were considered when modeling PCM fluids. A detailed description of the other boundary conditions can be found in Shah et al. [3].

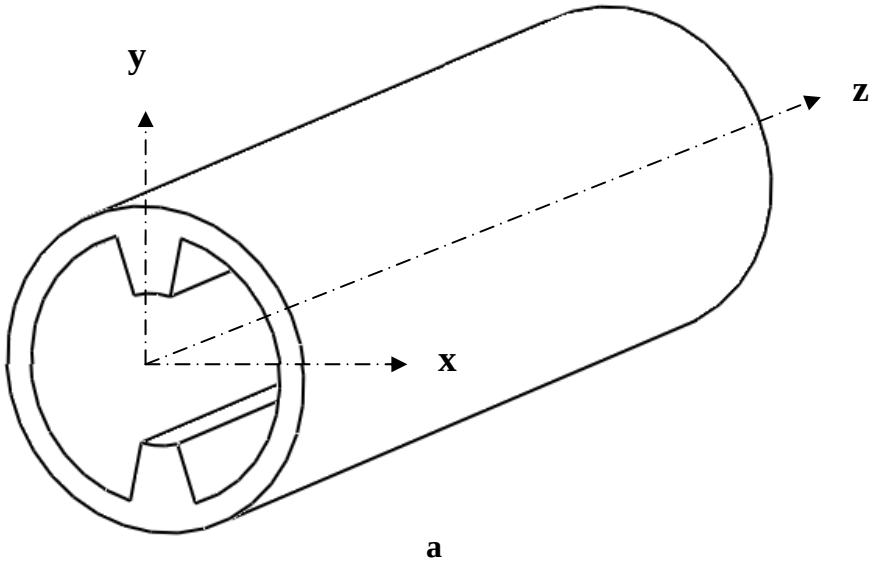

a

Fig. 5. H1 and H2 boundary conditions.

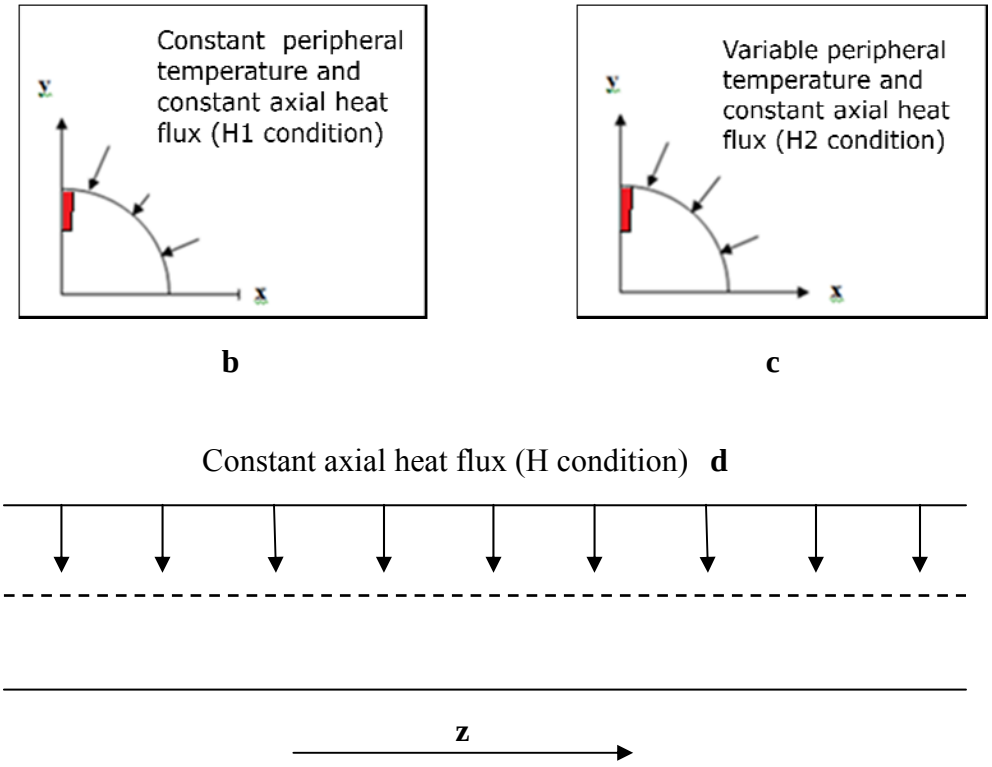

Fig. 5. continued.

Two constant heat flux boundary conditions were used including H1 and H2. The H1 condition as shown in Fig. 5 (constant peripheral axial temperature and constant axial heat flux) does not accurately represent the behavior of a fluid like water flowing in a finitely thermally conducting finned tube under constant heat flux boundary condition. This is because the H1 (constant axial heat flux) condition assumes a uniform peripheral temperature that varies with axial distance. In reality there is a temperature distribution along the peripheral surface of the tube when water is in contact with a finitely thermally conductive fin. On the other hand, the H2 boundary condition is used for materials with low thermal conductivity values and non-circular ducts under a constant heat flux boundary condition. Both boundary conditions are illustrated in Fig. 5. Thus it was

decided to model the internally finned tube with the H2 boundary condition to observe the temperature distribution on the peripheral surface of the finned tube. The effect of two distinct fin thermal conductivity values including, one equal to the bulk thermal conductivity of the PCM fluid, and one equal to that of aluminum were considered with and without PCM fluid.

3.4 Flow and heat transfer parameters

Several parameters were identified and selected for the study. The following subsections describe how each parameter value was chosen.

3.4.1 Reynolds number

Reynolds number is a dimensionless number which is used to characterize different flow regimes such as laminar and turbulent. It is defined as the ratio of the inertial forces to the viscous force of a fluid. Since the problem under consideration is laminar is nature, the Reynolds number was fixed along with the diameter of the tube. The corresponding velocity was determined using Eq. (7). In case of a PCM, the Reynolds number is calculated based on the properties of the slurry rather than the properties of the individual phases.

$$Re_b = \frac{\rho w_{avg} D}{\mu} \quad \text{or} \quad Re_b = \frac{2r\, w_{avg}}{\upsilon_b} \tag{7}$$

The entry length requirements for a fully hydrodynamically and thermally developed flow in case of a smooth circular tube are given in equations (8)-(10) [28].

$$l_h = 0.054\,Re_d \cdot D \tag{8}$$

$$l_t = 0.054\,Re_d \cdot D \cdot Pr \tag{9}$$

$$Pr_b = \frac{\upsilon_b}{\alpha_b} = \frac{\rho_b c_{p,b} \upsilon_b}{k_b} \tag{10}$$

Where L_H, L_T, Pr_b are the thermal entry length for constant heat flux condition, constant wall temperature condition and the bulk Prandtl number. The Reynolds number and the diameter of the tube were carefully chosen to obtain an aspect ratio that can be easily modeled using a mesh generator (i.e. GAMBIT) and avoiding the use of slender elements.

3.4.2 Viscosity

The presence of microcapsules in the carrier fluid increases the viscosity of the slurry. The increase in viscosity is taken into account using Eq. (11).

$$\frac{\mu_b}{\mu_f} = \left(1 - c - 1.16c^2\right)^{-2.5} \tag{11}$$

Where, μb and μf are the bulk dynamic viscosity and the fluid dynamic viscosities.

3.4.3 Density

The density of the slurry is determined using Eq. (12). It is obtained by the volume averaged density of the individual components of the slurry material.

$$\rho_{sl} = c\rho_p + (1 - c)\rho_f \tag{12}$$

Where, ρ_{sl} is the bulk density of the PCM slurry.

3.4.4 Thermal conductivity

In the case of PCM fluid in laminar flow, there are two thermal conductivity models can be used. The first thermal conductivity model considers dilute suspension and can be calculated using the Maxwell's relation [2], Eq. (11). The second thermal conductivity model takes into account the interaction between the microencapsulated suspensions and the carrier fluid. As a result, there is an effective enhancement in the thermal conductivity of the overall fluid. This is taken into account by using a conductivity model based on the local particle Peclet number given in Eq. (12) and (13).

$$k_b = k_f \cdot \frac{2 + k_p/k_f + 2c\left(k_p/k_f - 1\right)}{2 + k_p/k_f - c\left(k_p/k_f - 1\right)} \tag{13}$$

$$f = 1 + BcPe_p^m = 1 + Bc8^m \left[Pe_f \left(\frac{r_p}{r} \right)^2 \right]^m \left[\frac{a}{r} \right]^m \tag{14}$$

$$B = 3.0, \quad m = 1.5, \quad Pe_p < 0.67 \tag{15}$$

$$B = 1.8, \quad m = 0.18, \quad 0.67 \le Pe_p \le 250 \tag{16}$$

$$B = 3.0, \quad m = \frac{1}{11}, \quad Pe_p > 250 \tag{17}$$

$$k_e = f \cdot k_b \tag{18}$$

Where, k_b, k_f, Pe_f, are the bulk thermal conductivity, carrier fluid thermal conductivity and the Peclet number of the carrier fluid. A user defined code calculates the thermal conductivity based on the Peclet number which returns a value to CFD

software FLUENT 6.3. The returned value is used in solving the energy equation. The user defined code is shown in the appendix A.

3.4.5 Specific heat

The specific heat of the PCM fluid takes into account the melting point and latent heat of fusion of the PCM as shown in Eq. (14) and (15).

$$Cp_b = Cp_{sl} = c_m Cp_p + (1 - c_m) Cp_f \text{ for } (T < T_1) \text{ and } (T > T_2) \quad (19)$$

$$Cp_e = (1 - c_m) Cp_f + \frac{c_m L}{(T_2 - T_1)} \quad \text{for } (T_1 < T < T_2) \quad (20)$$

Where, Cp_b and Cp_e are the bulk specific heat and the effective heat of the PCM fluid respectively. Fig. 4 shows the heat capacity behavior of Eq. (19) and (20) graphically. As it can be seen in Fig. 4, there is a significant increase in the specific heat capacity of the PCM fluid during the melting process (regime). It is to be noted that in case of a pure fluid, the difference between T_1 and T_2 is negligible or close to zero. Fig. 6 also shows that the effective specific heat capacity of PCM is higher than the specific heat of the carrier, and is assumed to remain constant throughout the melting process. Other specific heat functions (apart from rectangular) such as triangular and sinusoidal have been studied [18], and they seem to have no effect on the heat transfer numerical results during the melting process.

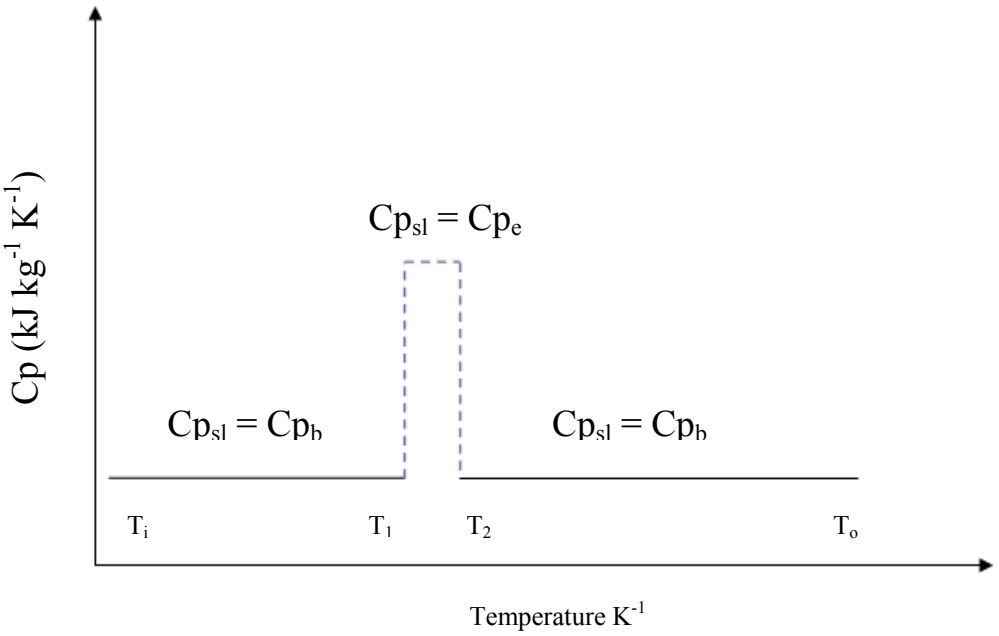

Fig. 6. Variation of specific heat with temperature.

3.4.6 Stefan number

In the study of PCM fluid, it is important to use a dimensionless parameter to capture crucial properties including particle loading and latent heat of fusion. The Stefan number is defined as the ratio of the sensible heat to the latent heat for a material. It is defined in two ways to satisfy two boundary conditions as in Eq. (21) and (22).

$$\mathrm{Ste}_{b,H} = \frac{c_{p,b} \cdot q''_w r \,/ k_b}{c_m \cdot L} \tag{21}$$

$$\mathrm{Ste}_{b,T} = \frac{C_b \left(T_w - T_m\right)}{cL\left(\rho_p / \rho_b\right)} \tag{22}$$

Where, $\mathrm{Ste}_{,b,H}$ and $\mathrm{Ste}_{b,T}$ are the Stefan numbers for the constant wall heat flux boundary and the constant wall temperature boundary condition.

3.4.7 Melting range

It is defined as the temperature range within which a material transforms from the solid to the liquid phase and vice versa. A pure substance has a unique melting point whereas a mixture melts through a range of temperature. In this study a melting rage of 0.07 is used to maintain computational stability while solving the phase change problem numerically. This assumption has been proven to be accurate when modeling phase change processes [17] and as it has been seen not to over- or under-predict the thermal performance of the PCM fluid significantly. The melting range for CHF and CWT boundary conditions are given in Eq. (23) and (24).

$$mr_H = \frac{T_2 - T_1}{q''_w r / k_b} \tag{23}$$

$$mr_T = \frac{T_2 - T_1}{T_w - T_i} \tag{24}$$

Where, mr_H and mr_T are the melting range for constant wall heat flux and constant wall temperature boundary conditions, respectively.

3.4.7 Sub-cooling range

It is the temperature range within which no phase change takes place. The phase change material begins to melt once sub cooling ends. In the present study, the sub cooling range has been assumed to be zero (i.e. the phase change process begins at the inlet of the tube). The sub-cooling range for CHF and CWT boundary conditions are given in Eq. (25) and (26).

$$ml_H = \frac{T_l - T_i}{q''_w r / k_b} \quad (25)$$

$$ml_T = \frac{T_l - T_i}{T_w - T_i} \quad (26)$$

Where, ml_H and ml_T are the sub-cooling ranges for constant wall heat flux and constant wall temperature boundary conditions, respectively.

3.4.9 Velocity profile

In all the cases that were studied, first the fully developed velocity profile was obtained by solving the laminar flow fluid problem with no heat transfer. This profile was used as inlet boundary condition to solve the thermally developing flow problem. The equation used as inlet velocity profile for a smooth tube is given below.

$$w = 2w_{avg}\left[1 - \left(\frac{a}{r}\right)^2\right]$$

Where, w and w_{avg} are the local and mean axial velocity of the PCM liquid in the tube.

3.4.10 Nusselt number

One of the main variables of interest is the Nusselt (Nu) number. Nu is a dimensionless measure of the convection heat transfer taking place inside a tube with flowing fluid. The Nusselt number for the H2 boundary condition is determined in a similar way to that of the H1 condition. In case of H2 condition the wall temperature is determined by taking the average of the temperature values on the local wall surface. In

general the Nusselt number for a constant heat flux boundary condition is given in Eq. (27).

$$Nu = \frac{q_w'' \times D}{(T_w - T_b) \times k_b} \tag{27}$$

$$T_b = \frac{\sum_{j=1}^{n} T_j \rho_j \left| \overrightarrow{\upsilon_j} \cdot \overrightarrow{A_j} \right|}{\sum_{j=1}^{n} \rho_j \left| \overrightarrow{\upsilon_j} \cdot \overrightarrow{A_j} \right|} \tag{28}$$

Where, Nu and T_b are the Nusselt number and the local bulk temperature, respectively. The Nusselt number for a constant wall temperature boundary condition is given in Eq. (29).

$$Nu_m = \frac{\bar{h} \cdot D}{k_b} \tag{29}$$

$$q = \bar{h} A \Delta T_{lm} \tag{30}$$

$$\Delta T_{lm} = \frac{T_m - T_z}{\ln\left[\frac{T_w - T_z}{T_w - T_m}\right]} \tag{31}$$

Where, Nu_m, T_{lm}, are the mean Nusselt number and the log mean temperature, respectively.

3.4.11 Peclet number

In previous studies [16], it has been shown that thermal conductivity can be enhanced by the microconvective effect caused by PCM particles in the carrier fluid. Those studies made use of the Peclet number to estimate the effective thermal conductivity. Peclet number is defined as the the ratio of advection to conduction of heat transfer rates in a fluid medium. The bulk Peclet number can also be defined as the product of the bulk Reynolds number and bulk Prandtl number in case of thermal diffusion. The equations for determining the bulk and the particle Peclet number are given in Eq. (32) and (33).

$$Pe_b = Re_b \times Pr_b \tag{32}$$

$$Pe_p = \frac{eD^2}{\alpha_f} \tag{33}$$

Where, Pe_b, Pe_p, e, are the bulk Peclet number, Particle Peclet number and velocity gradient, respectively.

3.4.12 Dimensionless temperature

Dimensionless temperature variables are used to facilitate the calculation of Nu. In this study, dimensionless temperature is defined as follows taking into account CHF and CWT boundary conditions as given in Eq. (26) and (27).

$$\theta_H = \frac{(T_m - T)}{(q_w r / k_b)} \tag{34}$$

$$\theta_T = \frac{(T - T_w)}{(T_m - T_w)} \tag{35}$$

Where, θ_H, θ_T are the dimensionless temperature for H and T boundary conditions.

3.5 Modeling procedure

In order to model the phase change material fluid thermal behavior computationally, a detailed modeling procedure was followed as shown in Fig. 7. The modeling procedure is based on standard heat transfer modeling where a particular geometry is meshed appropriately using a mesh generator. Then, boundary conditions are imposed and the before obtaining a stable numerical solution. The following sections explain in detail each part of the modeling procedure.

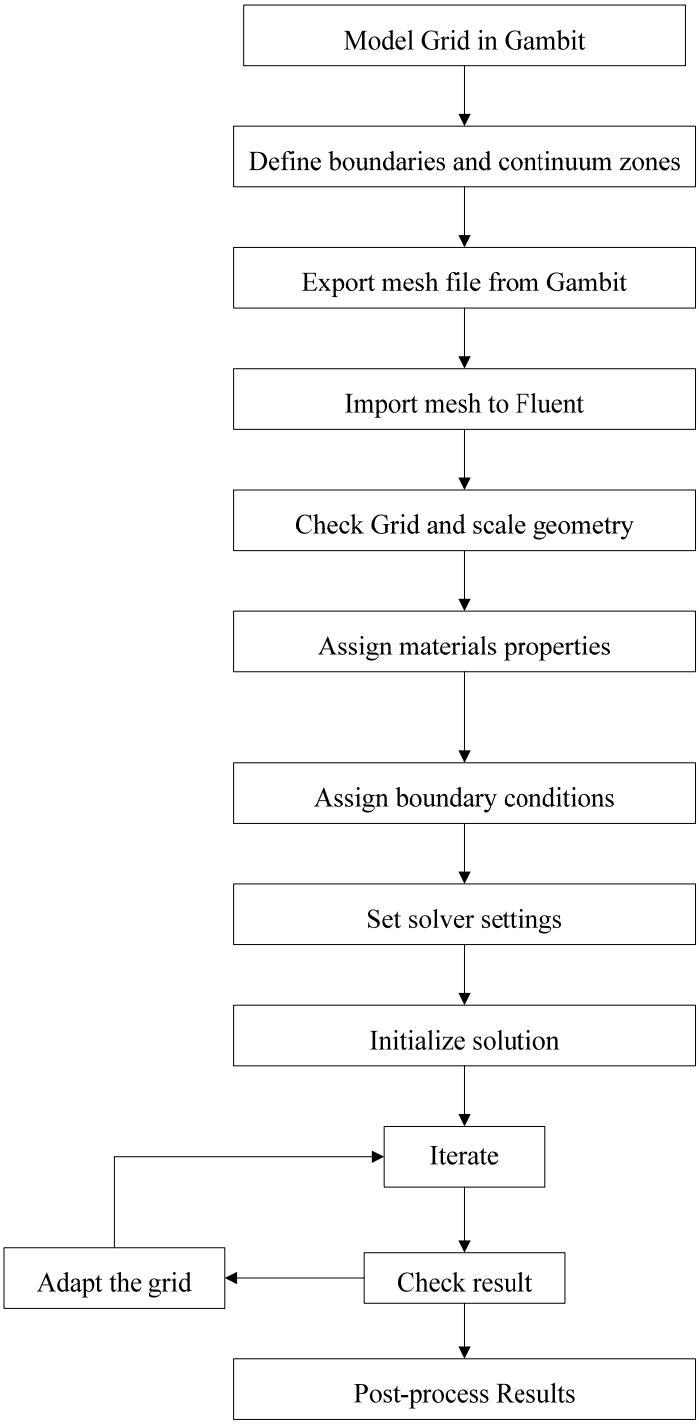

Fig. 7. Modeling and solution procedure.

3.6 Grid generation techniques

Two basic geometries were selected for the study. The first geometry consisted of smooth circular tube, while the second one was a circular tube with a two fins as illustrated in Fig. 1. Several meshing structures were considered and tested using simple boundary conditions. Then, the results were used to determine which meshing structure provided the most accurate results both in the case of smooth and finned tubes. The simulations pertaining to the smooth tube were solved as an axis-symmetric problem. It is known that there are high gradients in heat transfer coefficients in the entrance region of the tube. Thus it was decided to have the first mesh point on along the length of the tube at a dimensional distance of 10^{-4}. The dimensionless distance is calculated as shown in Eq. (36).

$$\zeta = z / (r.\mathrm{Re}_b \cdot \mathrm{Pr}) \qquad (36)$$

Where, ζ is the smallest dimensionless distance along the tube. Once the smallest length was determined, the length of the consecutive elements along the axis was gradually increased. This approach helped in capturing the high temperature gradients in the initial region of the tube. The radial direction of the tube was divided into 26 individual elements. Also the axial distance was divided into 20,000 individual elements. Boundary layer thickness equivalent to 1/100 of the pipe radius was used, and the thickness was gradually increased up to four layers with an incremental ratio of 1.25, using the boundary layer option in GAMBIT. The mesh distribution for a finned tube is shown in Fig. 8. The axial mesh distribution used in this case was similar to that of a circular tube. For the finned tube pure quadrilateral elements were used on the cross

sectional face of the geometry. The mesh distribution for each fin height case was altered slightly by increasing the number of peripheral points and reducing the number of radial points so as to get a fine mesh near the fluid-solid interface. The distribution (number of radial points x number of peripheral points) for each case is listed below.

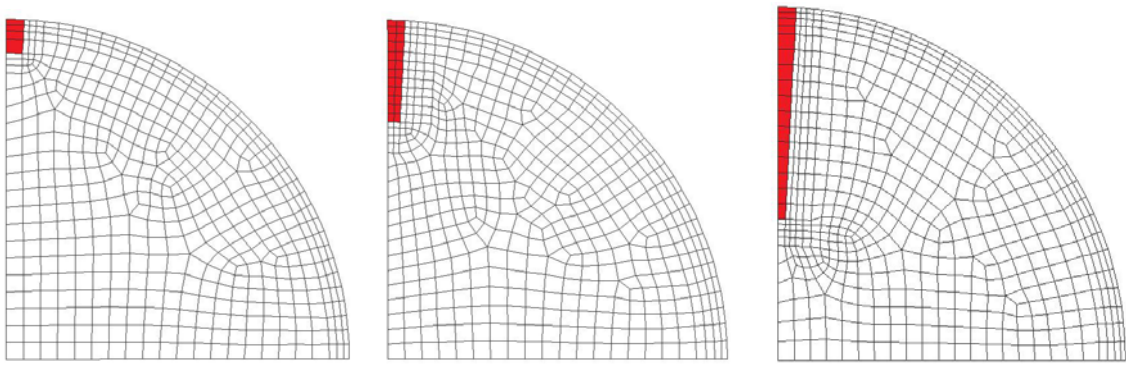

a (22 x 38) **b (22 x 34)** **c (24 x 32)**

Fig. 8. Mesh configurations.

3.7 Modeling using FLUENT 6.3

The internally finned tube with the phase change heat transfer phenomenon was solved as a three dimensional problem with a double precision solver. GAMBIT, a commercial mesh generating software was used to create the model for analysis in FLUENT 6.3 [27]. The default under relaxation factors provided in FLUENT 6.3 was used for momentum, pressure, energy calculations. In cases of low Stefan number, the under relaxation parameter for momentum and energy equation was reduced from 0.7 to 0.6, and 1.0 to 0.9, respectively. A second order discretization scheme was used to solve pressure, energy and momentum of the PCM fluid. The SIMPLE pressure-velocity

coupling algorithm was used to derive an equation for pressure from the discrete continuity equation. The continuity and the momentum equations were initially solved to get the fully developed velocity values for the smooth and the internally finned tube.

The fully developed velocity profile was set as a boundary condition at the inlet of the tube, and the problem was solved by assuming a hydrodynamically developed and thermally developing flow. Also, the convergence criterion for the continuity, momentum and energy equations was set to 10^{-6}. During post processing, Fluent was used to determine the wall temperatures and Tecplot was used to determine mass-averaged bulk temperature values at various cross sections in the smooth circular and internally finned tube. These values were used to calculate the local Nusselt number as shown in section 3.4.10. From appendix B to appendix F, it is explained how FLUENT's pre-processor, solver and post-processor, are used to obtain the desired results.

4. RESULTS AND DISCUSSION

4.1 Numerical validation

The numerical solutions are compared with analytical and previous numerical results in this section. Fig. 9 shows a dimensionless fully developed velocity profile for a single phase fluid in a circular tube. The results from the simulations agreed within 1% of the theoretical values for laminar flow. A fully developed velocity profile has been used to study the heat transfer performance of a smooth tube under laminar flow conditions. Then, the numerically-obtained Nusselt (Nu) number value of a circular tube was validated using known Nu number correlation for water under constant wall heat flux boundary condition. The numerical result for the Nusselt number was within 1% of the closed-form analytical solution [28]. The results are shown in Fig. 10.

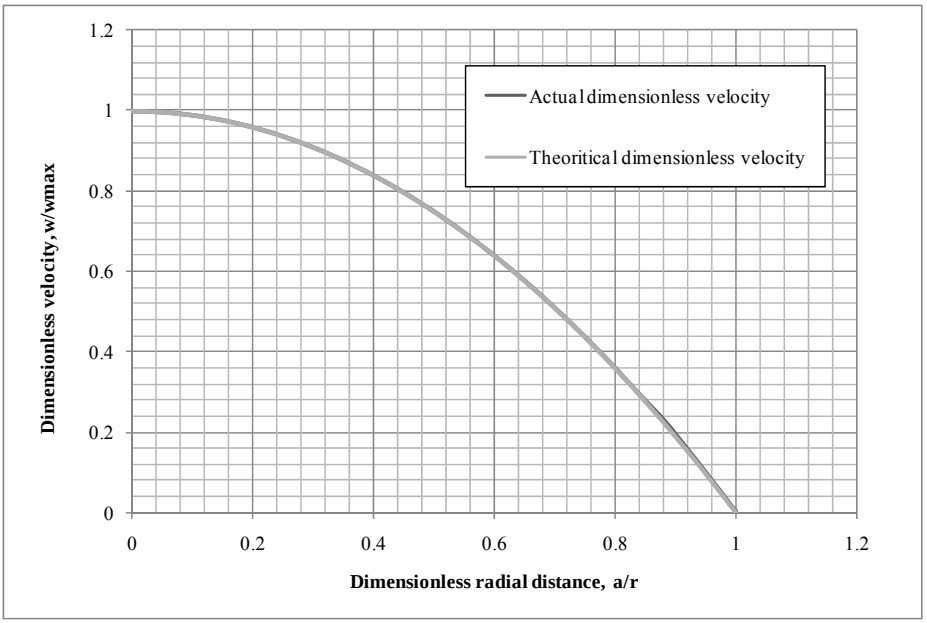

Fig. 9. Dimensionless fully developed velocity profile.

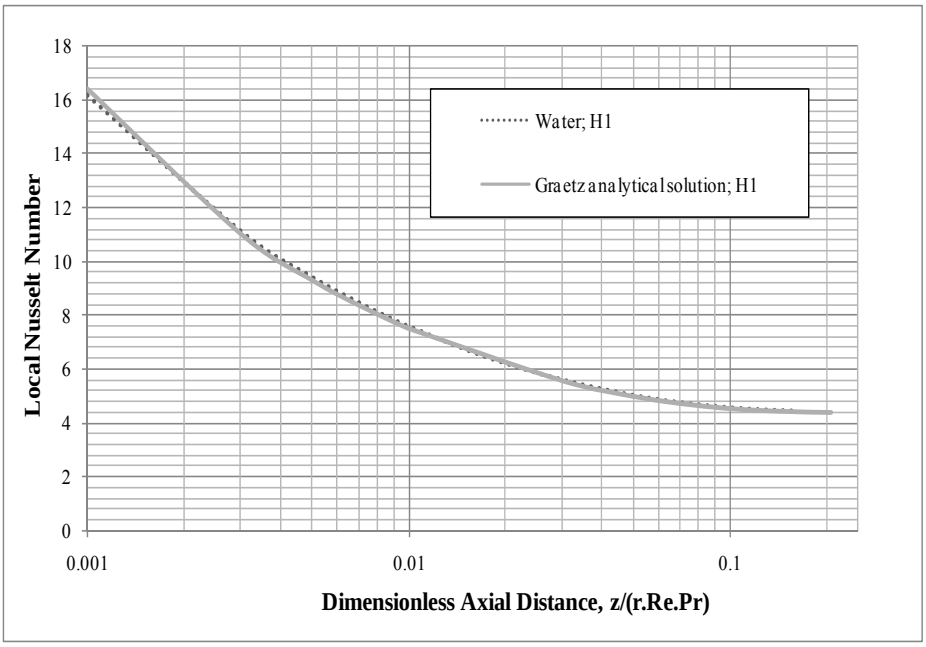

Fig. 10. Validation local nusselt number for circular duct.

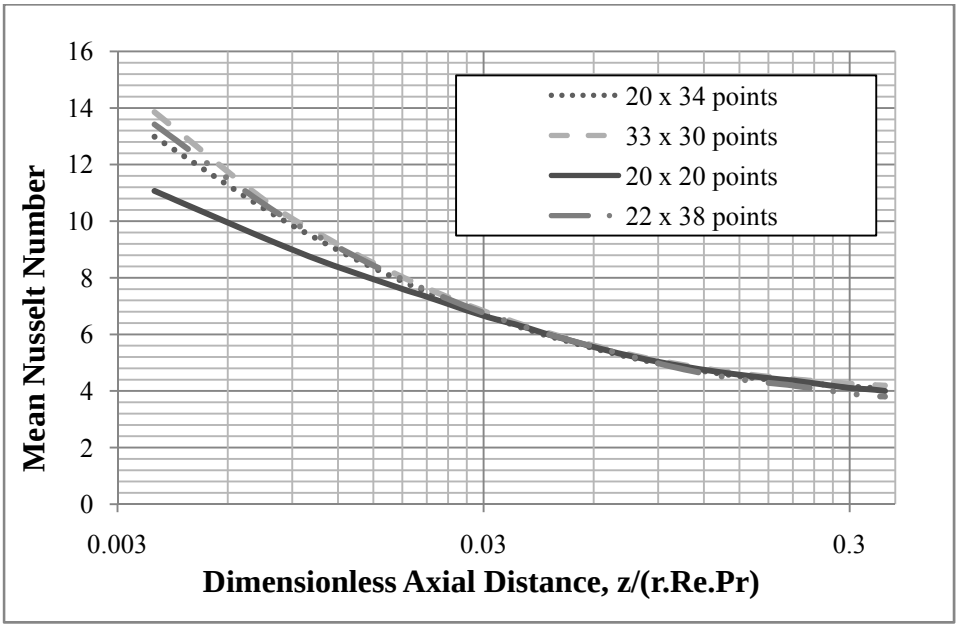

Fig. 11. Validation of mean nusselt number for a finned tube, H=0.1, CWT.

Several mesh distributions were analyzed to determine the optimum number of points in the radial and circumferential direction of the finned tube by using a single phase fluid. The results for four different mesh configurations including 20 x 20 and 33 x 30 are shown in Fig. 11. It was determined that a mesh configuration of 22 x 38 ($k_{,s} = k_{,Al}$) agreed with the results from Kettner et al. [5] within 3%. Furthermore, it became clear that finer mesh configurations provided similar results.

Then the analysis of a PCM fluid was carried out using a two dimensional model of the tube. The results of Stefan number equal to 5, (denoted by Ste = 5 in the graph) with a melting range of 10^{-4} (denoted by mr = 0.0001in the graph) and using the enhanced thermal conductivity model (denoted by k,sl = k,e in the graph) was found to be within 3% of the literature values [16]. The comparison is shown in Fig. 12.

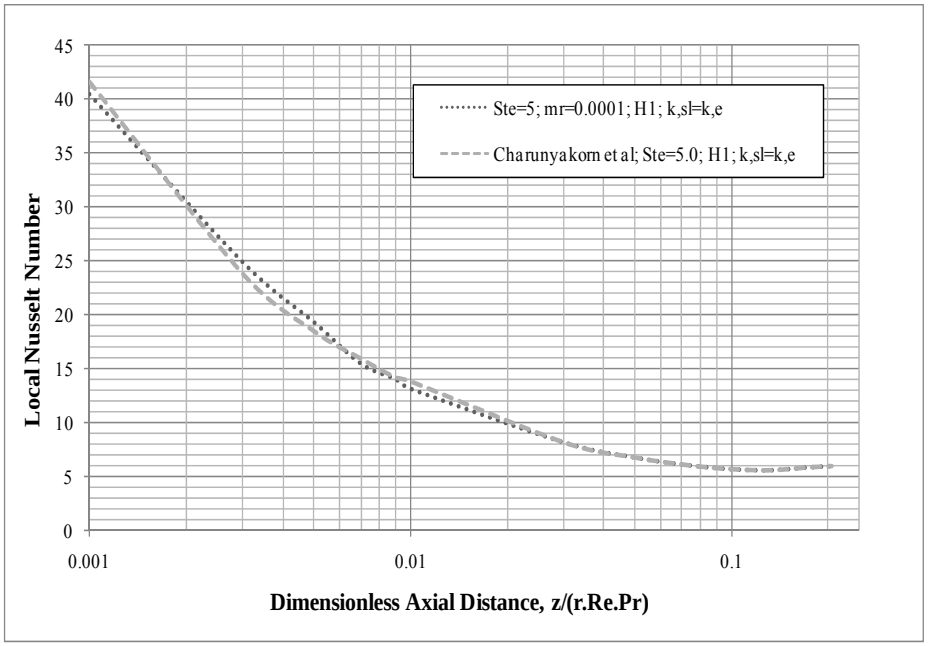

Fig. 12. Validation of nusselt number during phase change process.

A detailed parametric study was performed by varying the Stefan number, melting range, thermal conductivity of the fluid. The results are shown in Fig. 13. It was observed that the value of the local Nusselt number increased as the value of Stefan number was decreased. The melting range of 10^{-4} was used to represent the zero melting range exhibited by a phase change material. The results indicate that the local Nusselt Number is 1.25 to 2 times higher than that of the single phase fluid in the entrance region. It can be seen that the local Nusselt number decreases until the phase change process is complete, and then slightly rises to reach a constant value. This can be attributed to the temperature profile which is not fully developed at the end of the phase change process. The Nusselt number stabilizes to a constant value once the temperature profile is fully developed. With higher the concentration of the PCM particles or lower the Stefan number, the longer it takes for the PCM fluid to reach a thermally fully developed condition.

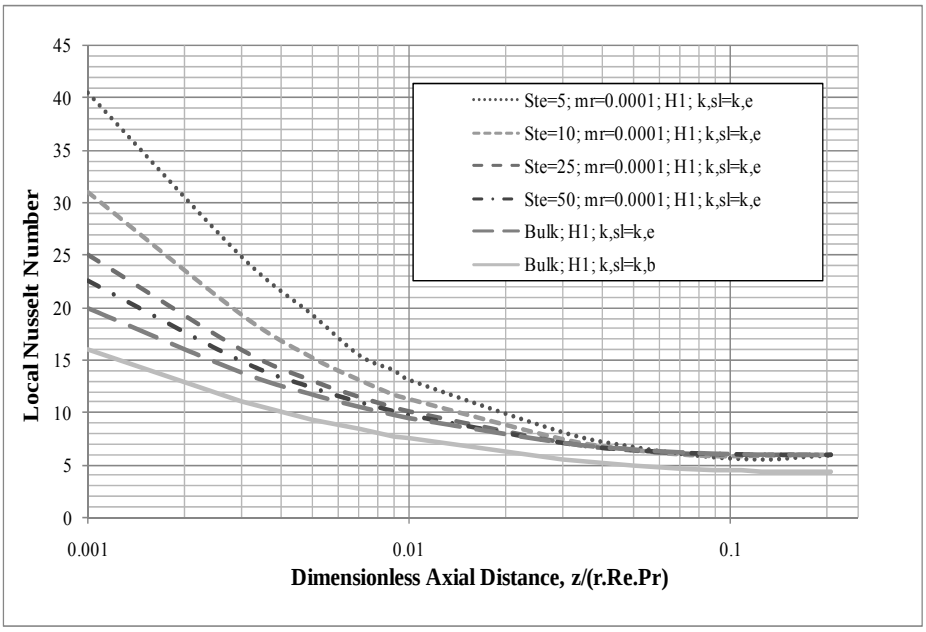

Fig. 13. Variation of Nu with stefan number: $k_{,sl} = k_{,e}$.

The effect of the enhanced conductivity model based on the Peclet number is shown in Fig. 14. It can be seen that for a constant heat flux boundary condition (denoted by H1 in the graph) without phase change, the enhanced thermal conductivity model (denoted by k,sl = k,e) predicts a higher Nusselt number compared to using the bulk thermal conductivity of the fluid (denoted by k,s l = k,b). This is because the model takes into account the thermal conductivity enhancement due to micro convection [29].

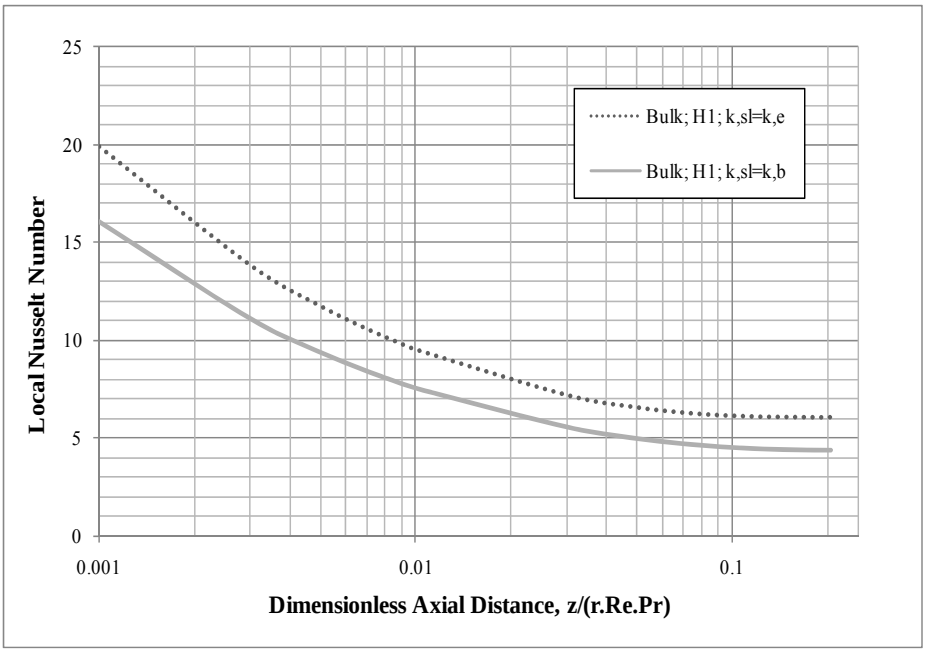

Fig. 14. Comparison of Nu using k_e and k_b without phase change.

The effect of Stefan number on the Local Nusselt number using the bulk conductivity of the fluid is shown in Fig. 15. It can be seen that the only difference is the magnitude of the values obtained in the two cases. This behavior can be attributed to the enhanced conductivity model.

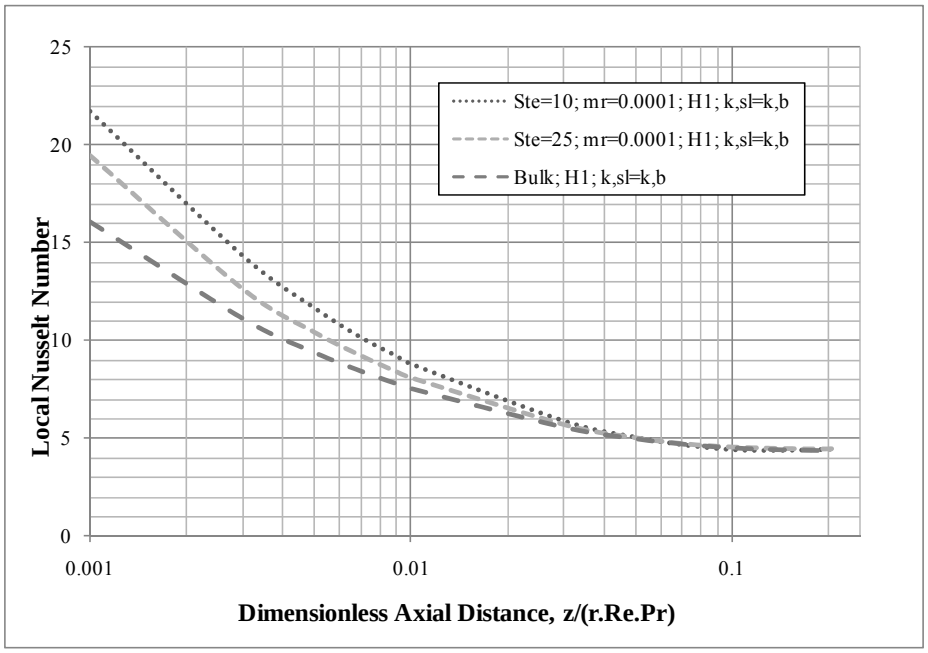

Fig. 15. Variation of Nu with stefan number: $k_{,sl} = k_{,b}$.

Fig. 16 shows the magnitudes of Nusselt number for two thermal conductivity models for a constant Stefan number. It can also be seen that at the end of the phase change process that corresponding fully developed Nusselt number based on the enhanced thermal conductivity model ($Nu_e = 6.0$), and the one based on bulk thermal conductivity model ($Nu_b = 4.36$) converge to the corresponding single-phase Nu number for each model.

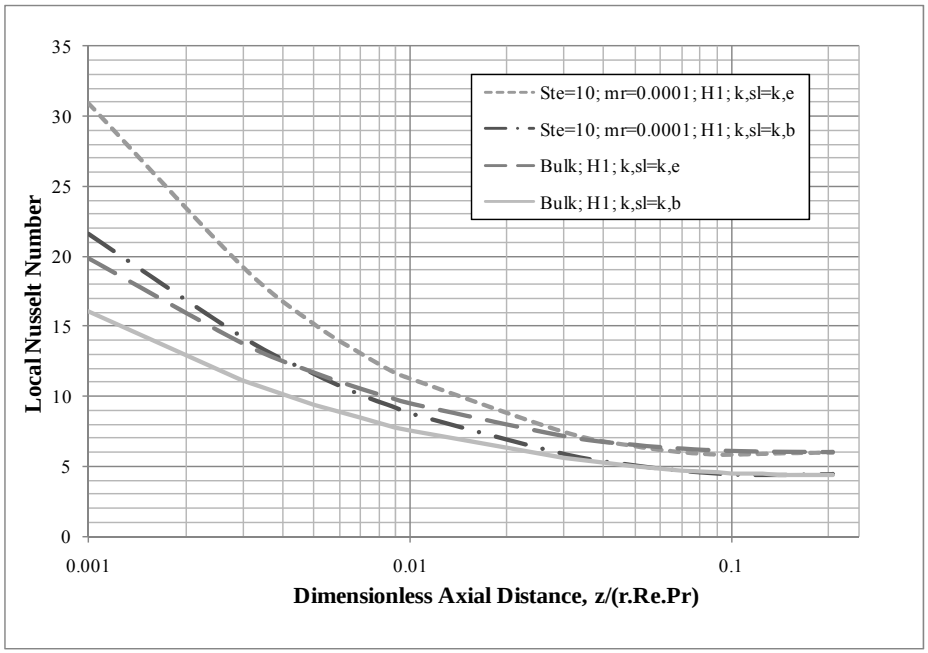

Fig. 16. Variation of Nu for varying Stefan number.

Several observations can be made from the results for the phase change process in smooth circular tubes. The enhanced thermal conductivity model based on the Pectlet number always predicted a higher value of Nusselt number than the thermal conductivity model based on the bulk fluid. This was attributed to the micro convective effects which were considered by the enhanced conductivity model. It was also noticed that for any given thermal conductivity model for the PCM fluid; a lower value of Stefan number predicts higher Nusselt number. Another observation was that the Nusselt number then increased and remained constant once the fully developed value was reached ($Nu_e = 6.0$ and $Nu_b = 4.36$).

4.2 PCM under fully developed hydrodynamically and thermally conditions

The effect of Stefan number and two different conductivity models on Nusselt number are presented in this section. The performance of PCM fluid with constant heat flux boundary condition (H1 boundary condition) under hydrodynamically and thermally fully developed conditions was considered. The flow conditions were set so that the melting process could start once the PCM fluid was hydrodynamically and thermally developed. Fig. 17 Shows Nusselt number values for varying Stefan number for melting range of 0.07. A close up figure of the same process can be seen in Fig. 18. Here it can be seen that the Nusselt number increased when the Stefan number was reduced.

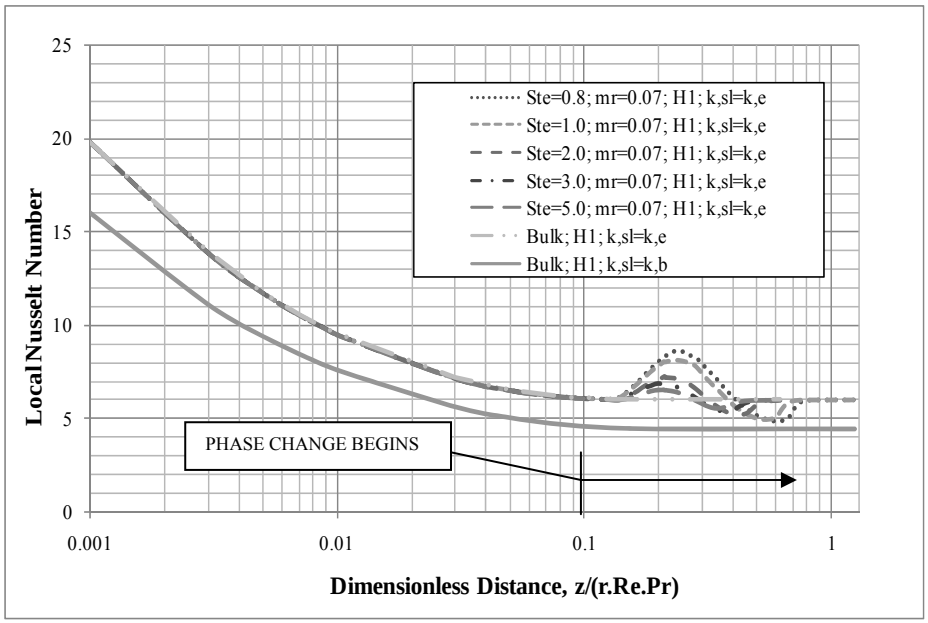

Fig. 17. Variation of Nu under thermally developed conditions: $k_{,sl} = k_{,e}$.

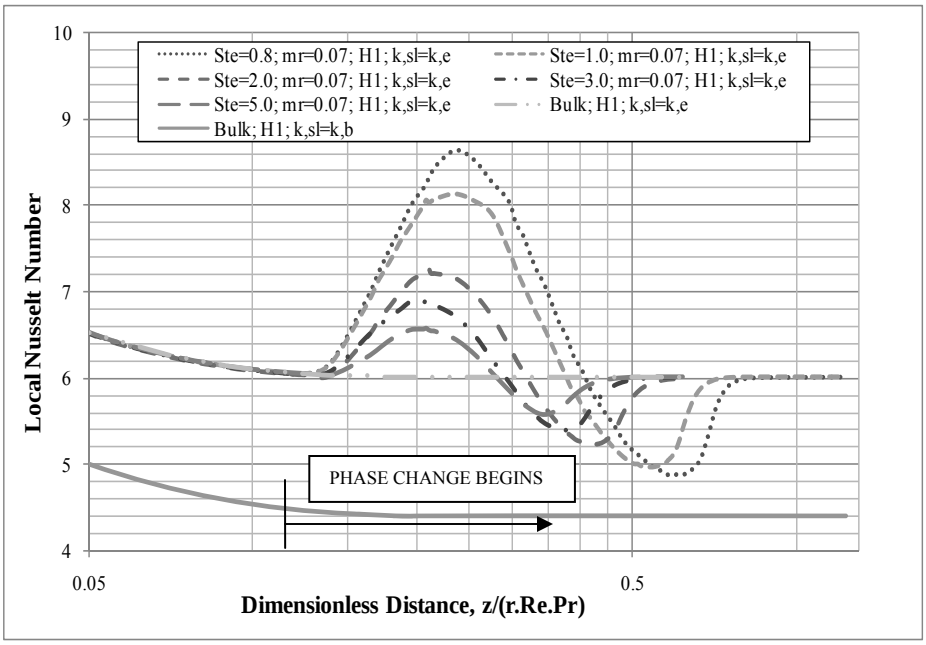

Fig. 18. Close up of Fig. 17.

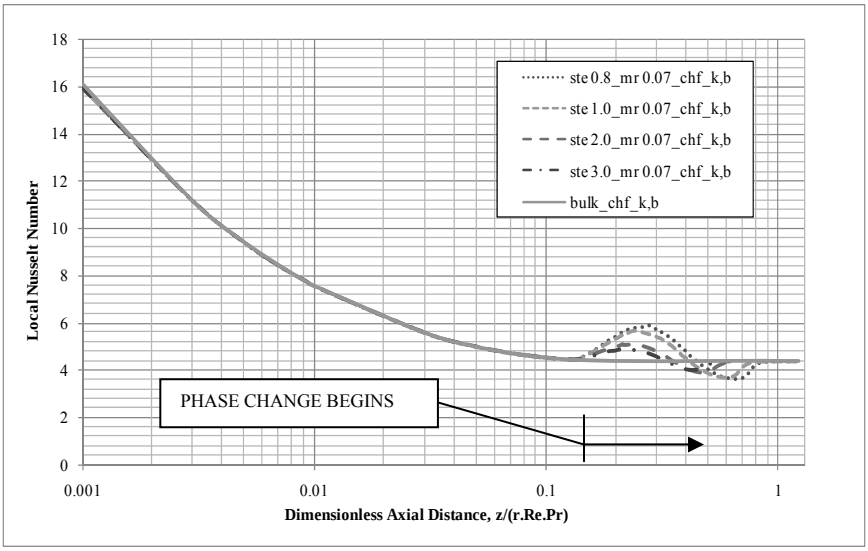

Fig. 19. Variation of Nu under thermally developed conditions: $k_{,sl} = k_{,b}$.

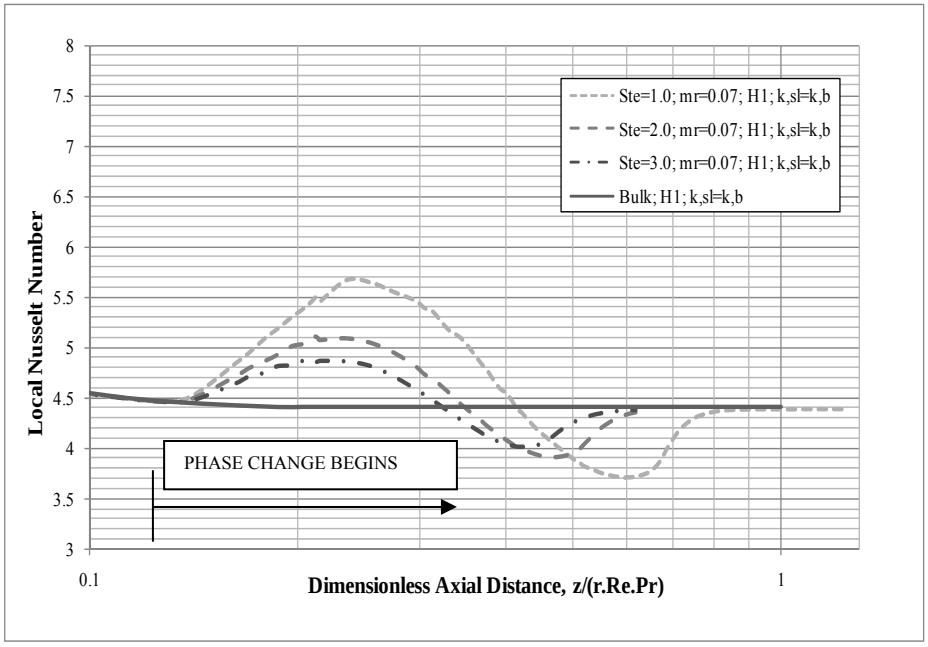

Fig. 20. Close up of Fig. 19.

In Fig. 18, it can be seen that the melting process first induce a positive increase in Nu number. As the melting process continues, the Nu number start decreasing until it reaches a minimum value. It can also be seen that as the Stefan number decreases, changes in the Nusselt number are more pronounced. Figs. 19 and 20 show the melting process under thermally fully developed conditions but using the bulk conductivity model. The phase change process followed the same trend as that seen in Figs. 17 and 18 with the magnitude of the Nusselt number varying due to the conductivity model used. The significant change in Nusselt number due to lower Stefan number can be explained using Fig. 21. When the phase change process begins at a dimensionless distance of 0.12, the difference between the wall temperature and the bulk temperature reduces

along the axis. This results in an increase in Nusselt number early in the phase change process. That difference increases due to partial melting of PCM particle near the tube wall which results in a decrease in Nusselt number. Finally when the phase change process is complete, the difference between the bulk and the wall temperature gradually reduces until it reaches a constant value, resulting in a constant Nusselt number after the phase change process is complete.

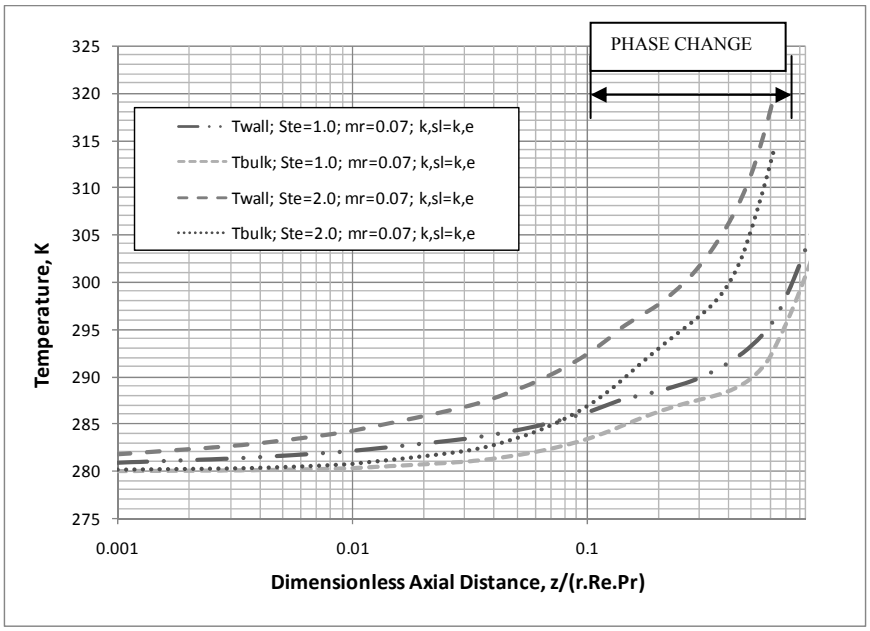

Fig. 21. Variation of T_w and T_b under thermally fully developed conditions.

Several observations were made during the study of the phase change process under hydrodynamically and thermally fully developed conditions. Higher Nusselt numbers were observed for tubes with a low Stefan number.

4.3 Internally finned tube with H2 boundary condition

The results of the internally finned tube with the H2 boundary condition are discussed in this section. The heat transfer performance of the tube with and without the phase change materials are also discussed in detail.

4.3.1 Single phase fluid in internally finned tube with H2 boundary condition

4.3.1.1 Flow and heat transfer characteristics

Fig. 22 shows the velocity contours for a finned tube with a height ratio of 0.1. It can be seen that the axial velocity is zero near the wall surfaces and maximum at the center of the tube.

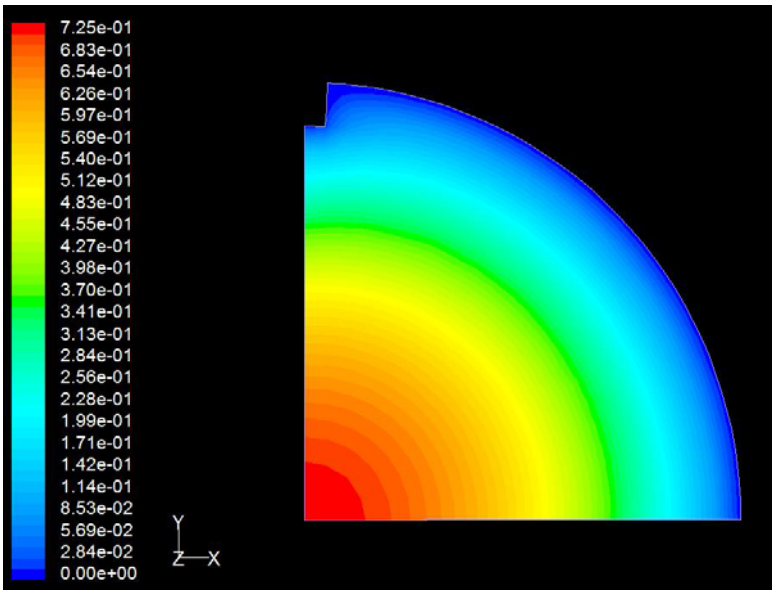

Fig. 22. Axial velocity contour for single phase fluid: H = 0.1

It can also be seen from Figs. 23 and 24 that as the fin height is increased, the maximum value of the axial velocity shifts away from the center of the tube.

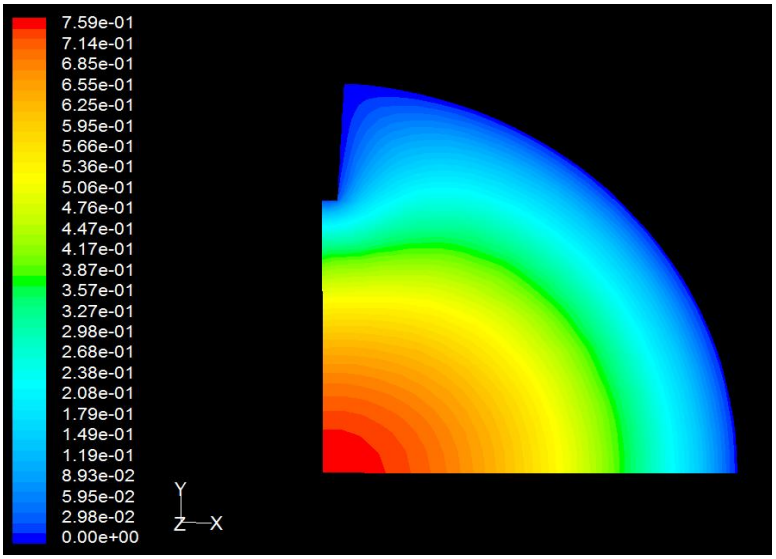

Fig. 23. Axial velocity contour for bulk fluid: H = 0.3.

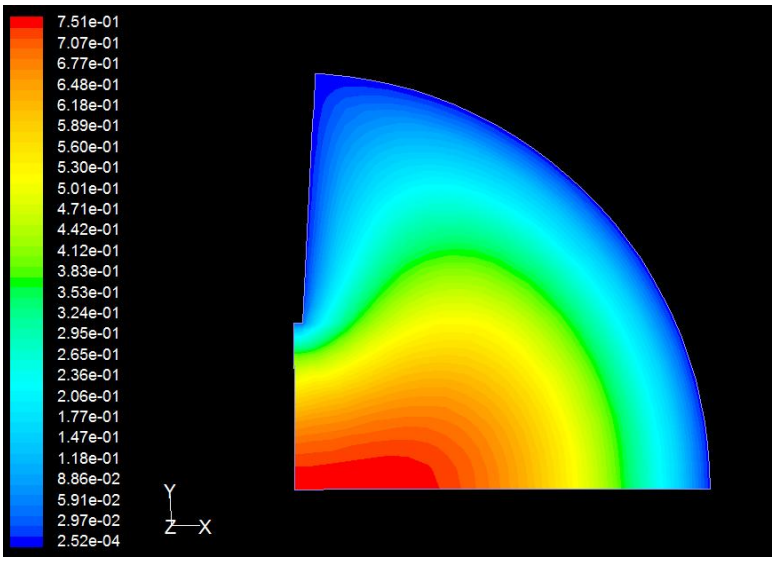

Fig. 24. Axial velocity contour for single phase fluid: H = 0.6.

If the fin height is further increased, it can be seen that the peak velocity shifts away from the center. This observation is consistent with the results from Kettner et al. [5]. The results obtained for Nusselt number during the hydrodynamically fully developed flow are given in Fig. 25. It can also be seen that the Nusselt number decreases along the tube length until a constant value is reached. This indicates that the fluid has reached its fully developed condition. It was found that for constant fin thermal conductivity (equal to that of the single phase fluid denoted by k,s=k,b in the graph) the fin height does not have a significant effect on the Nusselt number.

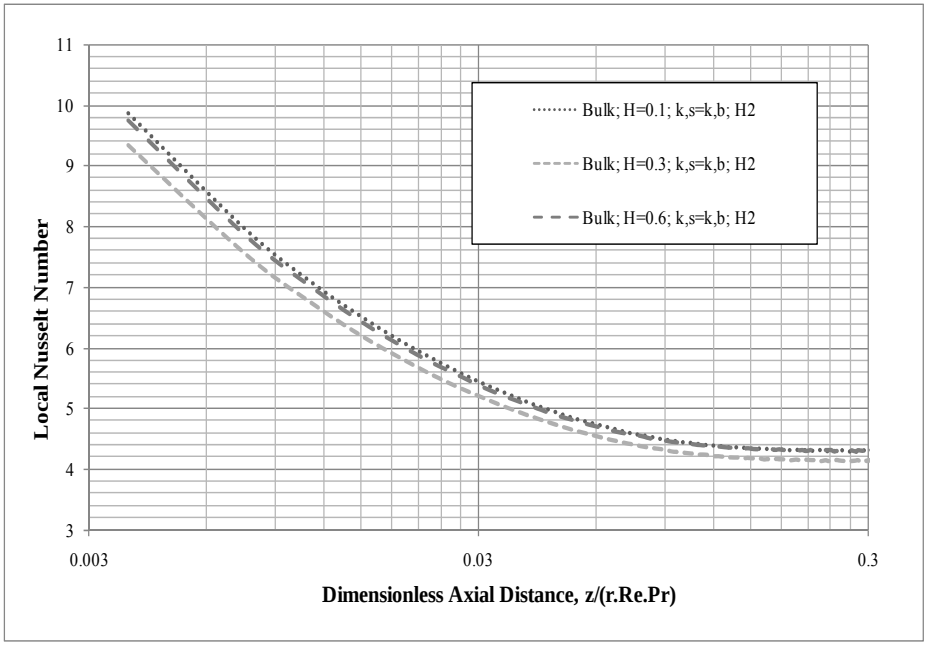

Fig. 25. Variation of Nu for single phase fluid: H = 0.1, 0.3, 0.6.

From Fig. 26 it is evident that Nusselt number increased by a significant value at higher fin height values. This is primarily due to the higher fin thermal conductivity (i.e.

equal to that of aluminum, denoted by k,s=k,Al in the graph). From Figs. 27- 29 it can be seen that a given fin height, fin thermal conductivity has a significant impact on Nu number. Furthermore, when fin height is 0.6 of the tube radius yields enhanced Nu number values not seen at lower fin height values. Also the difference in the Nusselt number values in the entrance of the tube was higher in case of H=0.6 than H=0.1 and 0.3.

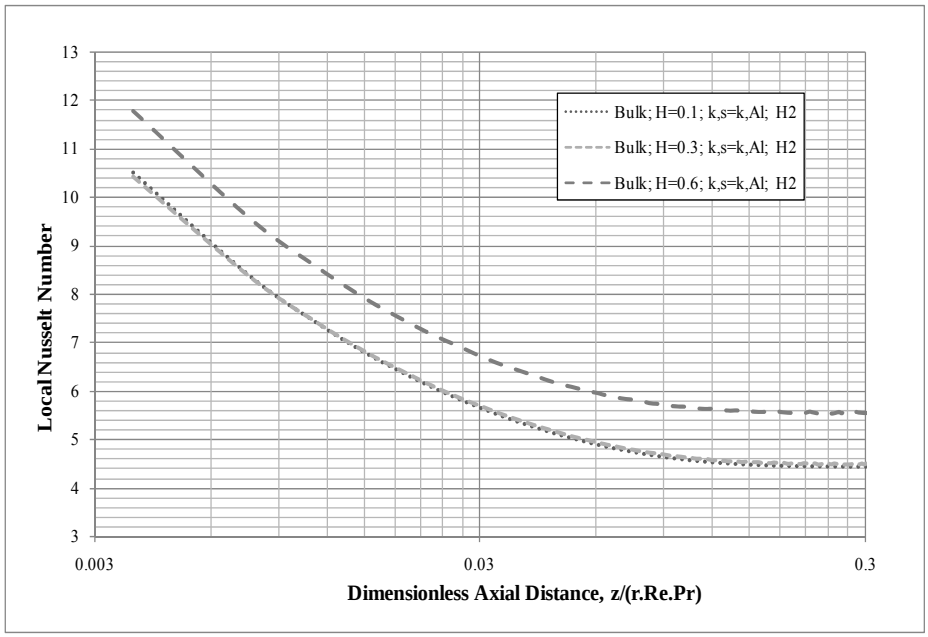

Fig. 26. Variation of Nu for single phase fluid: H = 0.1, 0.3, 0.6, $k_{,Al}$.

Thus it can be concluded that for a given fin height, a fin made of a material with higher thermal conductivity would yield better thermal performance than one with a lower thermal conductivity. Also the thermal performance of a higher fin is better than a

shorter one for the materials considered. This can be attributed to the higher internal surface area available for heat transfer.

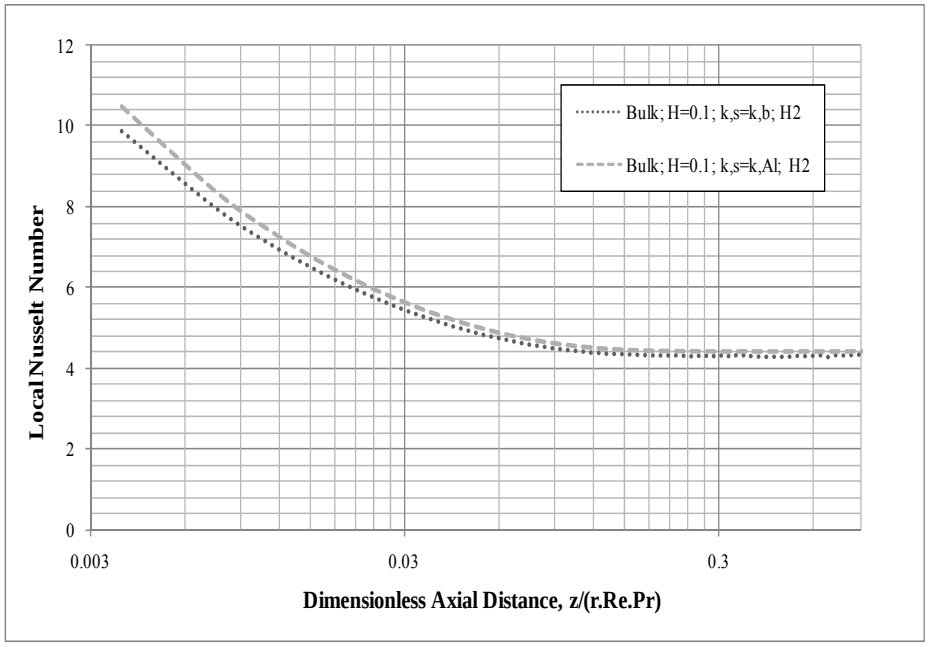

Fig. 27 Variation of Nu for single phase fluid: H = 0.1.

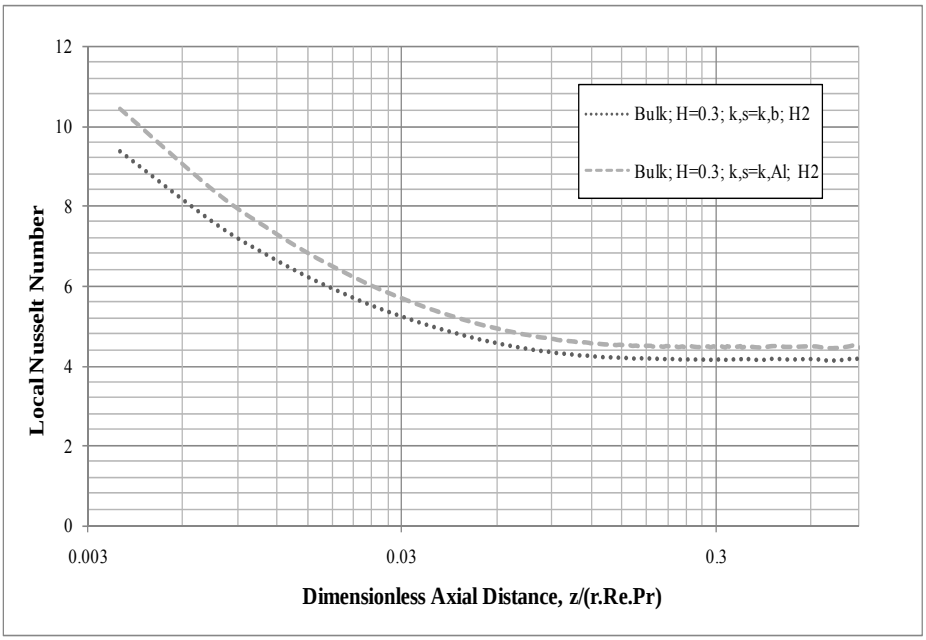

Fig. 28. Variation of Nu for single phase fluid: H = 0.3.

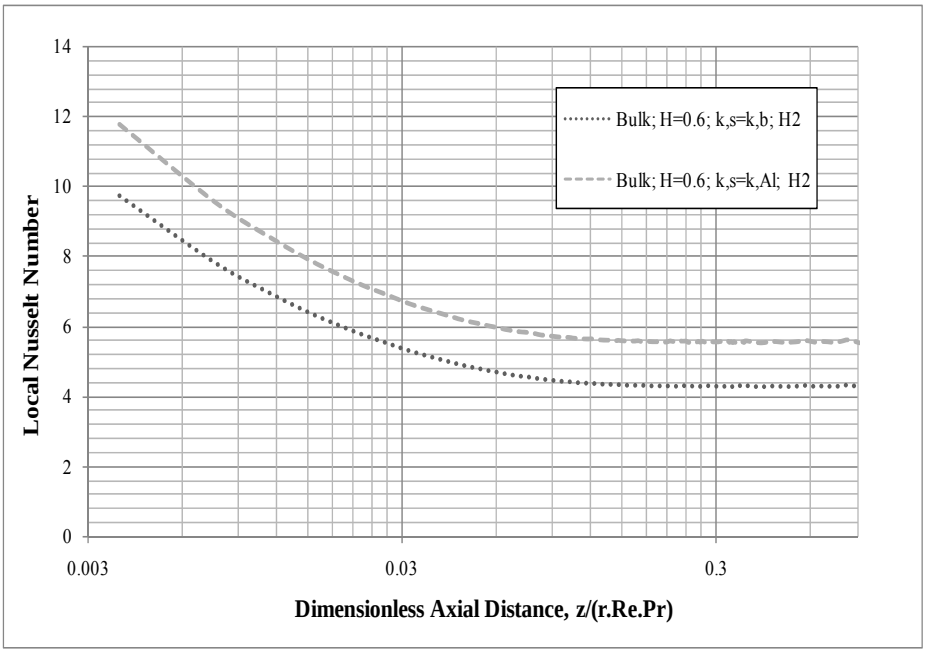

Fig. 29. Variation of Nu for single phase fluid: H = 0.6.

Several overall observations can be made from the analysis of a single phase fluid flowing through an internally finned tube under the H2 boundary condition. It is found that Nusselt number depends on two main factors, one being the fin thermal conductivity and the other being the fin height. For a constant fin height, tube with a higher fin thermal conductivity exhibit higher Nusselt number. Overall, it can be recommended that a higher (longer) fin with a high thermal conductivity be used to get the maximum performance out of a finned tube system. Another parameter influencing the performance of the finned tube is the number of fins. In this study, a tube with only two fins was considered. This is a critical parameter that should be considered to determine if it has a significant impact on the Nusselt than the results presented in this study.

4.3.2 PCM fluid in internally finned tube with H2 boundary condition

The effects of parameters like Stefan number, fin thermal conductivity and fin height on the thermal performance of the system are discussed in this section. Also the results were obtained for the Nusselt number under hydrodynamically fully developed flow and H2 conditions.

From Fig. 30, it can be seen that for a given Stefan number and thermal conductivity (equal to that of the bulk conductivity of the PCM fluid), the Nusselt number values were not affected by the fin height. A significant improvement was seen in the Nusselt number values for different fin heights when a higher conductivity (as that of aluminum) was used [Fig. 31]. Also the fully developed Nusselt number value was higher for a fin height ratio of 0.6 as compared to the other fin height ratios. The same

trend in Nusselt number is seen when a Stefan number of 3.0 is used instead of 1.0 by varying the fin height and the thermal conductivity of the fin [Figs. 32-33]. The Nusselt numbers in the above discussed cases were found to be strongly dependent on the Stefan number and the thermal conductivity of the fin. As seen in case of phase change in a circular tube, the local Nusselt number decreases until the phase change process was complete, then slightly increases and then remains constant.

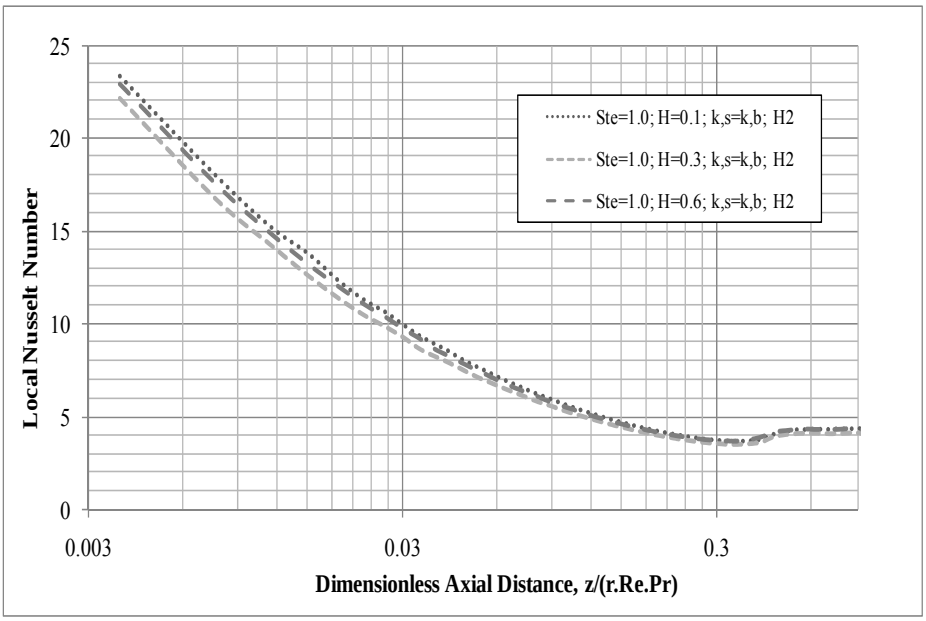

Fig. 30. Variation of Nu during phase change: Ste = 1.0, H = 0.1, 0.3, 0.6, $k_{,s} = k_{,b}$.

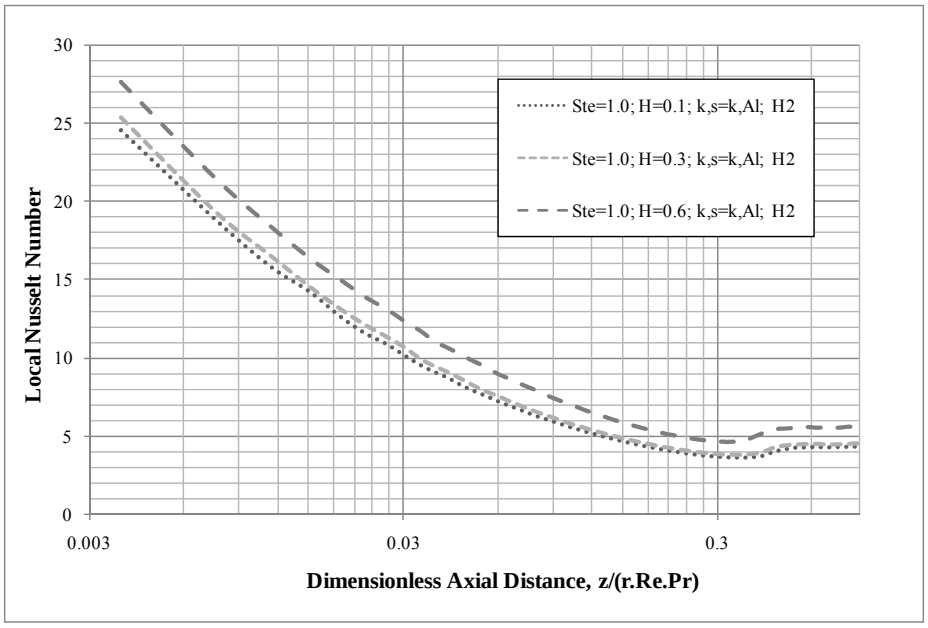

Fig. 31. Variation of Nu during phase change: Ste = 1.0, H = 0.1, 0.3, 0.6, $k_{,s} = k_{,Al}$.

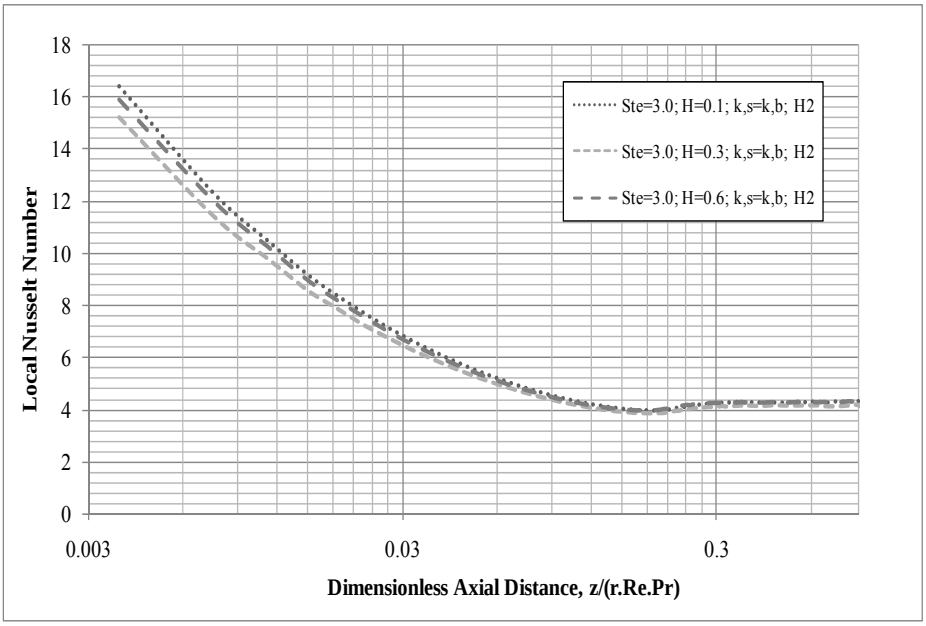

Fig. 32. Variation of Nu during phase change: Ste = 3.0, H = 0.1, 0.3, 0.6, $k_{,s} = k_{,b}$.

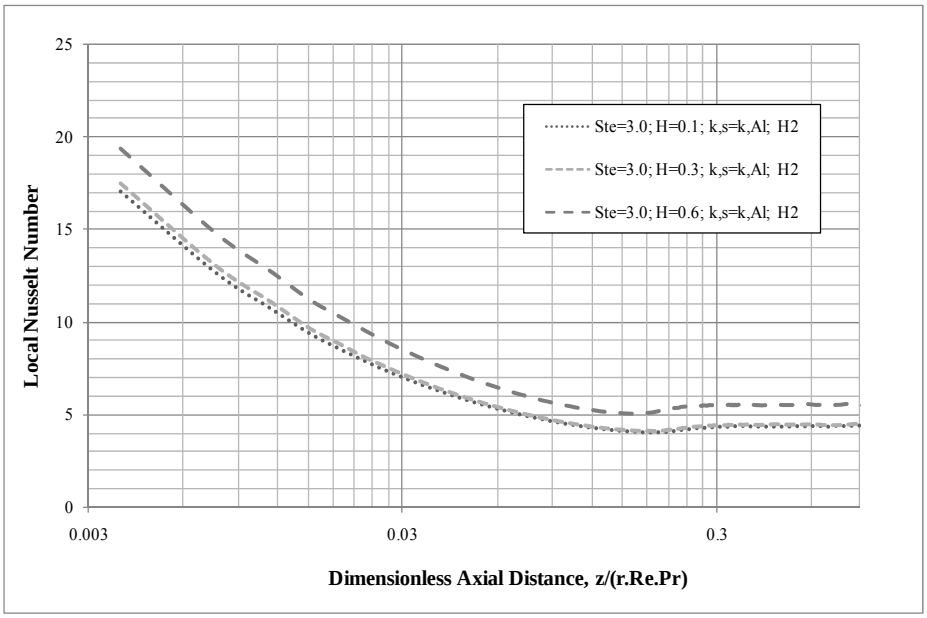

Fig. 33. Variation of Nu during phase change: Ste = 3.0, H = 0.1, 0.3, 0.6, $k_{,s} = k_{,Al}$.

The performance of the PCM fluid in an internally finned tube as compared to a single phase fluid flowing through a finned tube was evaluated. It was observed that for a given fin height and fin thermal conductivity, the PCM fluid had a higher Nusselt number compared to the single phase fluid with an internal fin of the same height. Also the PCM fluid with a lower Stefan number always had a higher Nusselt number compared to that of a higher Stefan number and the single phase fluid. Fig. 34 shows the performance of the internally finned tube for a fin thermal conductivity equal to that of the bulk thermal conductivity of the PCM fluid. It can be seen that the Nusselt number value of Stefan number of 1.0 is more than twice as that of the Nusselt number of the single phase fluid, and is almost 1.5 times as that of Stefan number of 3.0.

Similar trends in Nusselt number were seen for H = 0.3, 0.6, and the fin thermal conductivity equal to that of the single phase fluid. The Nusselt number was seen to be

larger when compared to the single phase fluid when a higher fin thermal conductivity (as that of aluminum) was used. Figs. 34-35 show the variation in Nusselt number for H = 0.1 and varying Stefan number. It was seen that the Nusselt number for Stefan number of 1.0 was higher than that of Stefan number equal to 3.0 and the single phase fluid at the same fin height ratio. Similar trends were observed for other fin height ratios, namely H = 0.3 and 0.6, when a higher fin thermal conductivity was used. Figs. 36-39 show the Nusselt number variation during the phase change process as compared to a single phase fluid, for different fin heights and fin thermal conductivity values.

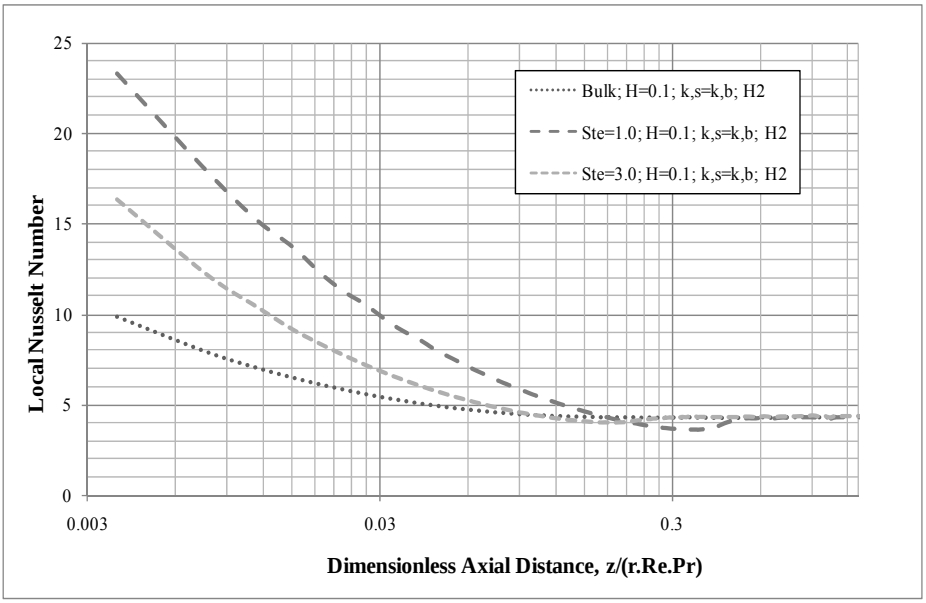

Fig. 34. Variation of Nu during phase change: H = 0.1, $k_s = k_{,b}$.

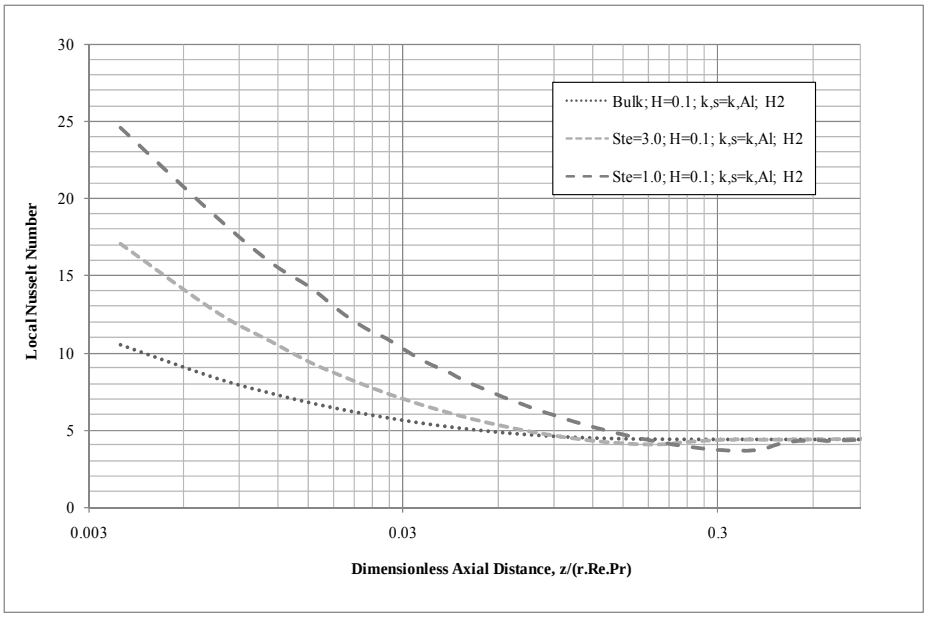

Fig. 35. Variation of Nu during phase change: H = 0.1, $k_s = k_{,Al}$.

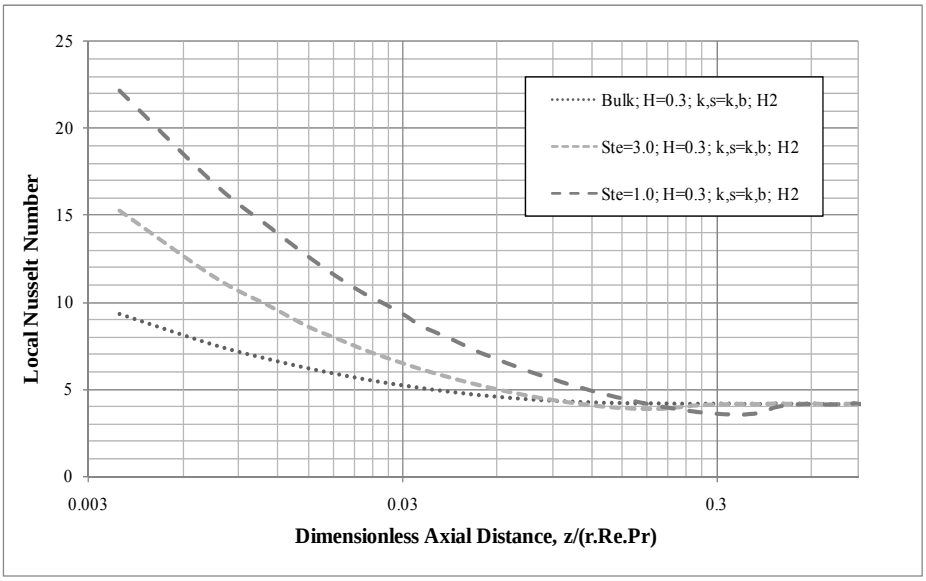

Fig. 36. Variation of Nu during phase change: H = 0.3, $k_s = k_{,b}$.

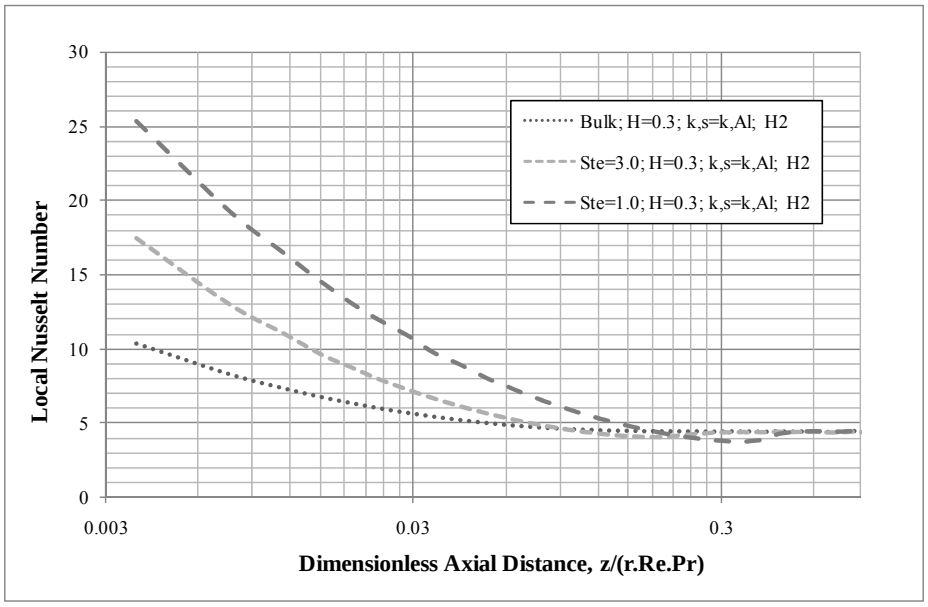

Fig. 37. Variation of Nu during phase change: H = 0.3, $k_s = k_{,Al}$.

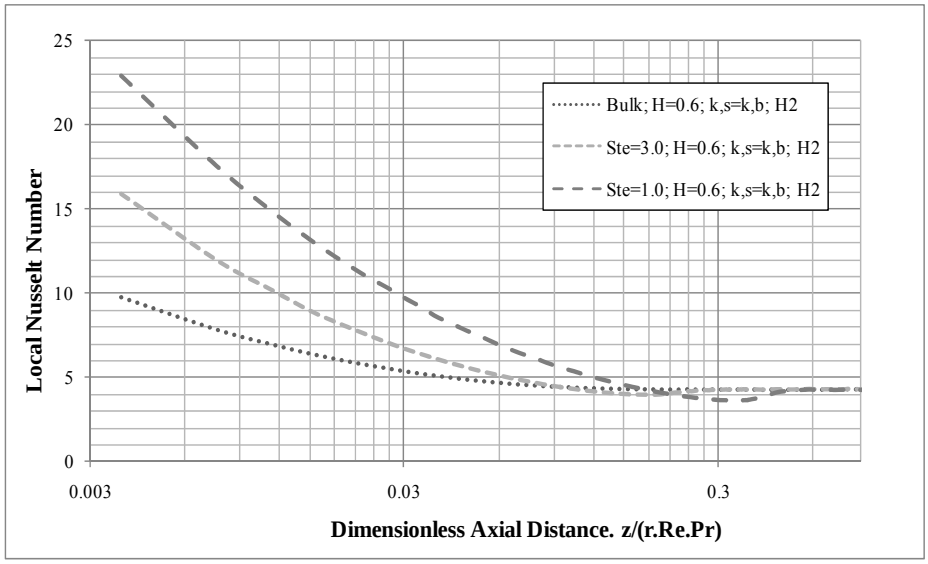

Fig. 38. Variation of Nu during phase change: H = 0.6, $k_s = k_{,b}$

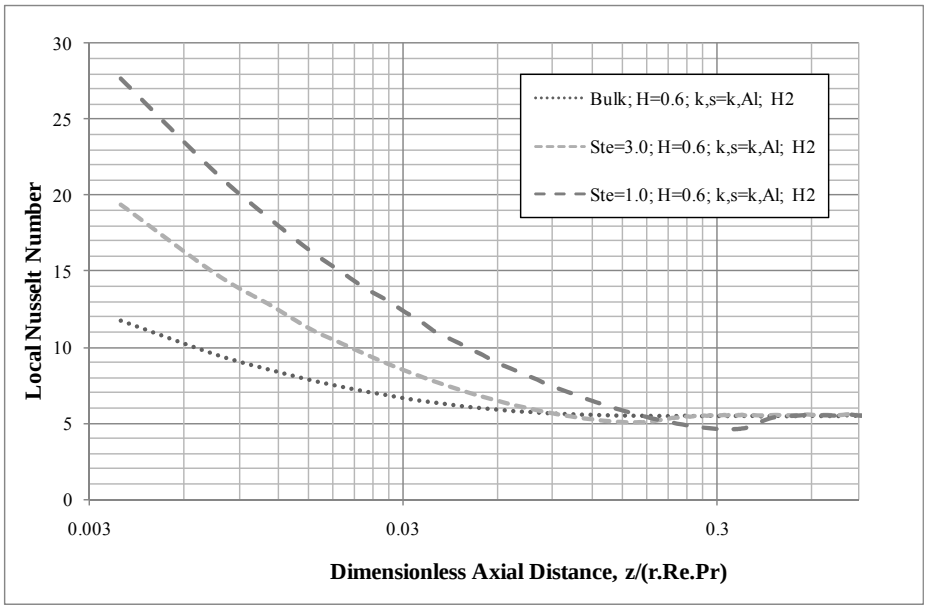

Fig. 39. Variation of Nu during phase change: H = 0.6, $k_s = k_{,Al}$

Several observations were made when the phase change process was modeled in an internally finned tube. An observation more relevant to the effect of the phase change process was that for any given fin thermal conductivity and fin height ratio, a lower Stefan number always seemed to predict a higher Nusselt number. This is a valid observation as a lower Stefan number predicted a higher Nusselt number even in case of a smooth circular tube. Also it was found that the Nusselt number reduced beyond its fully developed value once the phase change process was completed. The Nusselt number then increased and remained constant once the flow was thermally fully developed. This result is again consistent with the result obtained for a phase change process in a smooth circular tube. Another valuable observation was that the results of the phase change process in a finned tube cannot be compared to that of the phase

change process in a smooth circular tube as both the tube configurations are under different boundary conditions.

4.4 Internally finned tube with CWT boundary condition

The effects of parameters like Stefan number and fin height on the performance of the finned tube as studied in case of the CWT boundary condition will be discussed in this section. It was found that the above mentioned parameters had a similar impact on the Nusselt number as it was seen in the H2 boundary condition. The results were obtained for the Nusselt number under hydrodynamically fully developed flow conditions.

As it was observed from H2 boundary condition that a higher fin thermal conductivity significantly increased the Nusselt number, it was decided to consider only a fin thermal conductivity of that of aluminum in case of the CWT boundary condition. The Nusselt number variation for an internally finned tube, without phase the change process is shown in Fig. 40 It can be seen that for a fixed fin thermal conductivity, the fin height ratio was found to be a dominant parameter in influencing the value of the Nusselt number. A significant increase in Nusselt number (both in the entrance and fully developed regions) can be seen in case of H = 0.6 as compared to H = 0.1 and 0.3. As discussed in case of the H2 boundary condition, another important parameter influencing Nusselt number is the number of fins which is not done as a part of this study.

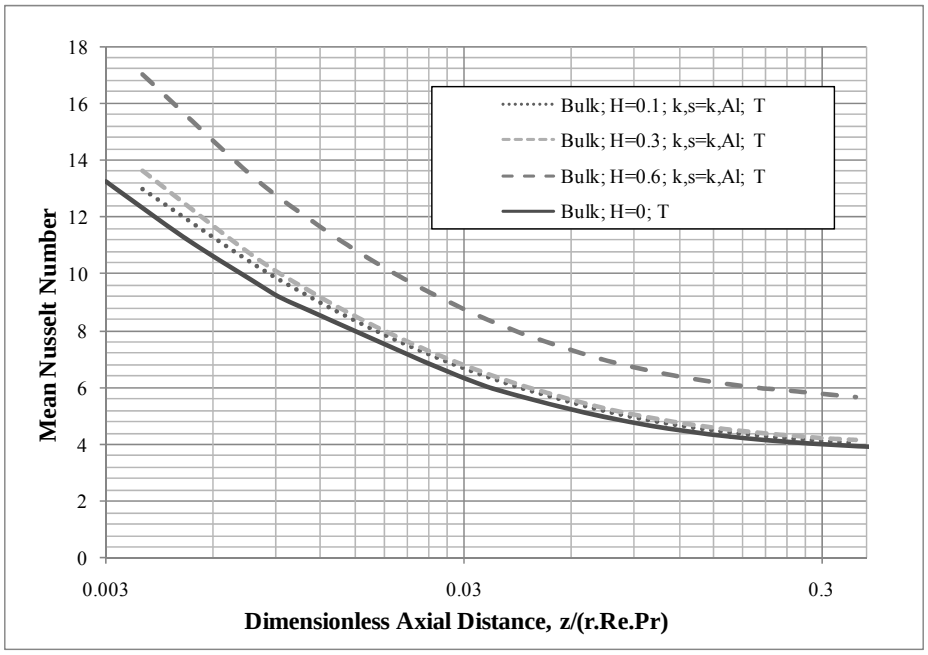

Fig. 40. Variation of Nu for single phase fluid under CWT boundary condition.

The effects of different fin height ratios (H = 0.1, 0.3, 0.6) during the phase change process of PCM fluid are discussed in this sub section. For a given Stefan number and fin thermal conductivity (equal to that of the aluminum), a significant improvement was seen in the Nusselt number values for all fin heights as compared to the Nusselt number for the single case fluid without fins. It was observed from Fig. 41 that the fin height ratio of 0.6 performed better than other fin height ratios. This is attributed to the higher surface area and enhanced thermal diffusion in the finned tube.

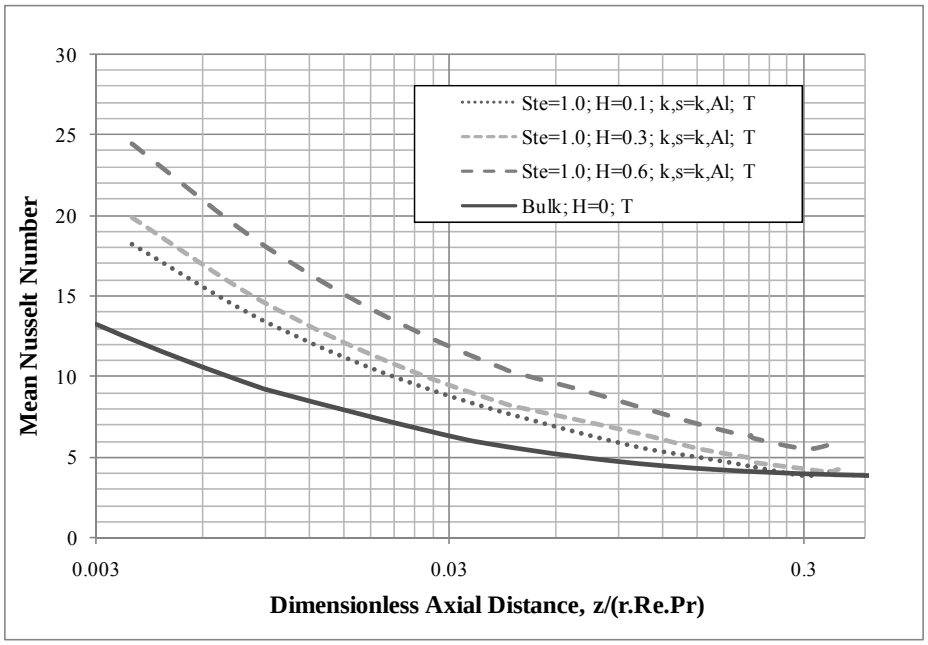

Fig. 41. Variation of Nu during phase change.

Figs. 42-44 compare the performance of different fin heights with phase change material fluid with that of the finned tubes carrying a single phase fluid. It was found that the finned tube with a phase change material fluid always performed better than the finned tube carrying a single phase fluid.

It was also observed that as the fin height ratio was increased, the relative performance of the finned tube with the phase change material as compared to the finned tube carrying a phase change material also increased.

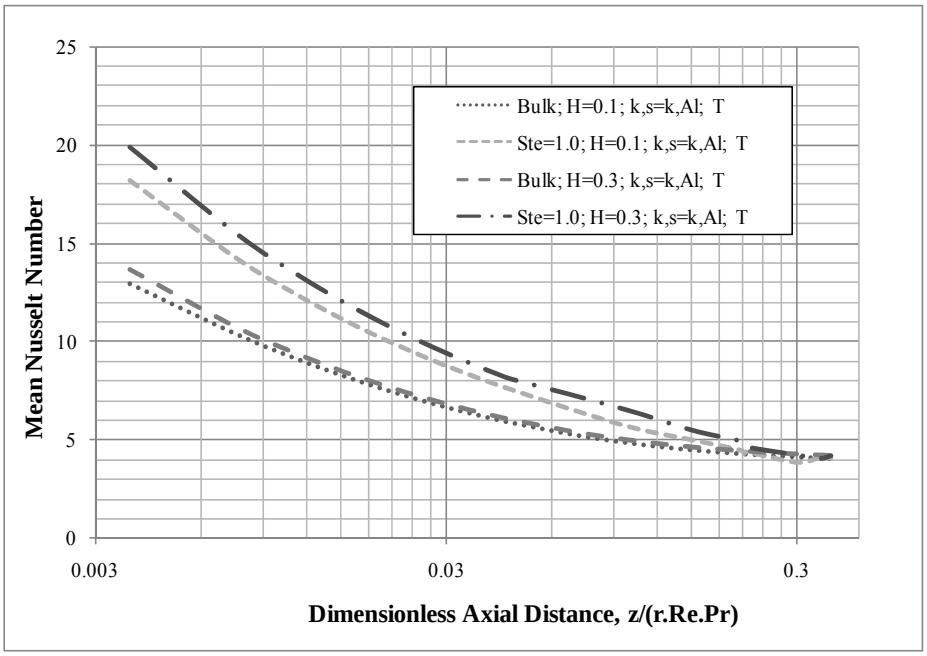

Fig. 42. Variation of Nu during phase change: CWT BC, H=0.1, 0.3.

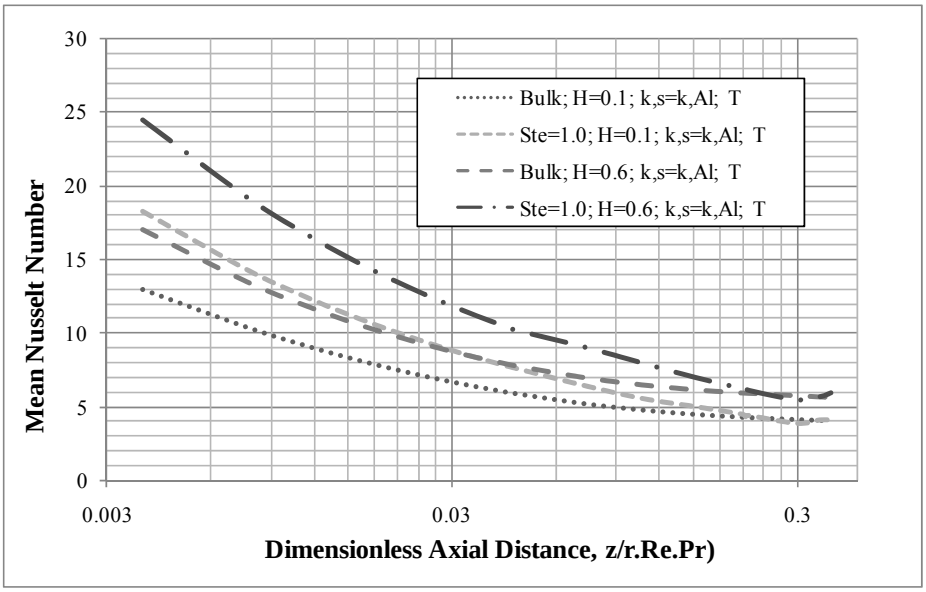

Fig. 43. Variation of Nu during phase change: CWT BC, H=0.1, 0.6.

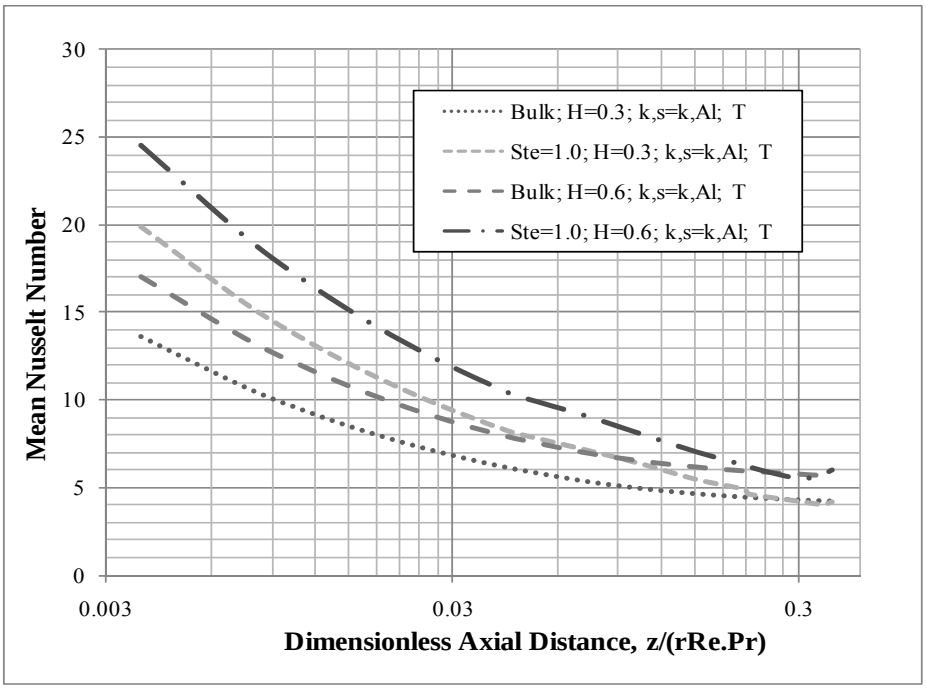

Fig. 44. Variation of Nu during phase change: CWT BC, H=0.3, 0.6.

The observations made during this study indicate that the fin height ratio has a significant impact on the performance of the internally finned tube when a phase change material is used. It can also be concluded that the Stefan number and the number of fins also significantly influence the Nusselt number in the entry region of the tube. The number of fins was also expected to increase the Nusselt number in the thermally fully developed condition.

5. CONCLUSION

The smooth circular tube and the internally finned tube were modeled using an effective specific heat technique to evaluate the heat transfer performance of a phase change material fluid. Two different boundary conditions, namely the constant wall heat flux condition with axially and peripherally uniform heat flux and a constant wall temperature condition were considered in the study. It was found that for the phase change material, the factors affecting the heat transfer performance in the smooth as well as the internally finned tubes were the single phaseStefan number, fin height and thermal conductivity. A significant increase (1.5 to 2 times than the single phase value for finned tubes with same fin height) in the heat transfer performance was obtained (H2 and T) when a height ratio of 0.6 was used. Also the increase in Nusselt number value was more pronounced when a fin thermal conductivity (equal to that of aluminum) was used. It was found that the trend in the Nuseelt number variation in case of H2 boundary condition was similar to that of the H1 boundary condition. The trends of the the Nusselt number curve for the T boundary condition also were found to be similar. The results for phase change material melting under thermally and hydrodynamically fully developed conditions indicate that after the phase change process is complete, the Nusselt number reduces beyond its fully developed values and then increase to again remain constant. The predictions made by the simulation is similar to what was expected in the sense that internally finned tubes enhanced the performance of the PCM fluid compared to a PCM fluid undergoing phase change process in a smooth circular tube. But experimental data

is needed to validate the results presented in the current study. The current study has considered only the laminar nature of the problem, for 15.0% of the PCM particles. Thus the effect of a higher volumetric concentration on the thermal performance has to be studied both under laminar and turbulent conditions for an internally finned tube taking into account the temperature dependence of viscosity and density so as to simulate the real problem.

REFERENCES

1. R.K. Shah, A.L. London, Thermal boundary conditions and some solutions for laminar duct flow forced convection, ASME Journal of Heat Transfer 96 (1974) 159–165.

2. J. C. Maxwell, A Treatise on Electricity and Magnetism, third ed., Vol. 1, Dover, New York, 1954, pp. 440-441.

3. Trupp, A. C., Soliman, H. M., Performance optimization of internally finned tubes for laminar flow heat exchangers, Heat Exchangers - Theory and Practice, Hemisphere Publishing Corporation, New York, 1983, pp. 899-916.

4. C. Prakash, Y.D. Liu, Analysis of laminar flow and heat transfer in the entrance region of an internally finned circular duct, ASME Journal of Heat Transfer 107 (1985) 84–91.

5. Kettner, I.J., Degani, D., Gutfinger, C., Numerical study of laminar heat transfer in internally finned tubes, Numerical Heat Transfer, Part A, 20 (1991) 159-180.

6. O. Zeitoun, A.S. Hegazy, Heat transfer for laminar flow in internally finned pipes with different fin heights and uniform wall temperature, International Journal of Heat and Mass Transfer 40 (2004) 253–259.

7. I.M. Rustum, H.M. Soliman, Numerical analysis of laminar forced convection in the entrance region of tubes with longitudinal internal fins, ASME Journal of Heat Transfer 110 (1988) 310–313.

8. J.H. Masliyah, K. Nandakumar, Heat transfer in internally finned tubes, ASME J. Heat Transfer 98 (1976) 257–261.

9. H.M. Soliman, The effect of fin material on laminar heat transfer characteristics of internally finned tubes, in: Chenoweth JM, Kaeilis J, Michel JW, Shenkman S (eds) Advances in Enhanced Heat Transfer, ASME, New York, Book No. 100122, 1979

10. H.M. Soliman, A. Feingold, Analysis of fully developed laminar flow in longitudinal internally finned tubes, Chem. Eng. J. 14 (1977) 119–128.

11. H.M. Soliman, A. Feingold, Analysis of heat transfer in internally finned tubes under laminar flow conditions, Proceedings of the 6th International Heat Transfer Conference, Vol. 2, 1978, pp. 571-576.

12. H.M. Soliman, T.S. Chau, A.C. Trupp, Analysis of laminar heat transfer in internally finned tubes with uniform outside wall temperature, ASME J. Heat Transfer 102 (1980), 598–604.

13. C.R. Swaminathan, V.R. Voller, A time-implicit filling algorithm, Appl. Math. Modelling 18 (1994) 101–108.

14. E. Assis, L. Katzmann, G. Ziskind, R. Letan, Experimental and numerical investigation of phase change in a spherical enclosure, Proceedings of 4th European Thermal Sciences, National Exhibition Centre, Birmingham, United Kingdom, March, 2004, pp. 29–31.

15. L.C. Tao, Generalized numerical solutions of freezing a saturated liquid in cylinders and sphere, AIChE Journal 13 (1967) 165–169.

16. P. Charunyakorn, S. Sengupta, S.K. Roy, Forced convection heat transfer in microencapsulated phase change material slurries: flow in circular ducts, International Journal of Heat and Mass Transfer 34 (3) (1991) 819–833.

17. Y. Zhang, A. Faghri, Analysis of forced convection heat transfer in microencapsulated phase change material suspension, Journal of Thermophysics and Heat Transfer 9 (4) (1995) 727–732.

18. Alisetti EL, Roy SK. Forced convection heat transfer to phase change materials slurries in circular ducts, Journal of Thermophysics, 14 (1999) 115-118.

19. S.K. Roy, B.L. Avanic, Laminar forced convection heat transfer with phase change material emulsions, International Communications in Heat and Mass Transfer 28 (7) (2001) 895-904.

20. Hu, X., Zhang, Y., Novel insight and numerical analysis of convective heat transfer enhancement with microencapsulated phase change material slurries: laminar flow in a circular tube with constant heat flux, International Journal of Heat and Mass Transfer 45 (2002) 3163–3172.

21. B. Niezgoda-Zelasko, W. Zalewski, Momentum transfer of ice slurry flows in tubes, modeling, International Journal of Refrigeration 29 2006 (3) 429-436.

22. E. Choi, Y.I. Cho, H.G. Lorsch, Forced convection heat transfer with phase-change-material slurries: turbulent flow in a circular tube, International Journal of Heat and Mass Transfer 37 (1994) (2) 207–215.

23. M.S. Goel, S.K. Roy, S. Sengupta, Laminar forced convection heat transfer in microcapsulated phase change material suspensions, International Journal of Heat and Mass Transfer 37 (4) (1994) 593–604.

24. X. Wang, J. Niu , Y. Li, Y. Zhang , X. Wang , B. Chen , R. Zeng , Q. Song, Heat transfer of microencapsulated PCM slurry flow in a circular tube, AIChE Journal 54 (4) (2008) 1110-1120.

25. Y. Yamagishi, H. Takeuchi, A.T. Pyatenko, N. Kayukawa, Characteristics of MPCM slurry as a heat transfer fluid, AIChE J. 45 (1999) 696–707.

26. M. Lacroix, Study of the heat transfer behaviour of a latent heat thermal energy storage unit with a finned tube, International Journal of Heat and Mass Transfer 36 (1993) 2083–2092

27. FLUENT 6.3 User's Guide, Fluent, Inc., Lebanon, NH, 2006.

28. P. Incropera, D. DeWitt, Fundamentals of Heat and Mass Transfer, fifth ed., John Wiley & Sons Inc. 2002.

APPENDIX A

User Defined Code

```
#include "udf.h"
#include <stdlib.h>

DEFINE_PROPERTY (xxhu_3d_k,q,t)
{  real kf,kp,kb,temp,c,pep,a,f,ke,x4[3],m;
 kf=0.60;
 kp=0.15;
 temp=1;
 c=0.15;
 C_CENTROID(x4,q,t);
 m=kp/kf;
 a=sqrt(pow(x4[0],2)+pow(x4[1],2));
 kb=kf*(2+m+(2*c*(m-1)))/(2+m-(c*(m-1)));
 pep=(8*temp*a/.01);
if(pep<.67)
   f=(1+(3*(pow(pep,1.5))*c));
if((pep>=.67)&&(pep<=250))
   f=(1+(1.8*pow(pep,.18)*c));
if(pep>250)
   f=(1+(3*pow(pep,(1/11))*c));

 ke=f*kb;
 return ke;
}
```

APPENDIX B

Pre-processor

The pre-processor is the initial stage of defining all the fluid flow inputs for a flow problem. The various aspects of this stage are listed below:

1. Characterization of the geometry

It is the region of interest in the computational domain. In the current problem it is the smooth and internally finned tubes.

2. Mesh generation

Mesh generation is the process of subdividing the domain into a number of smaller and non-overlapping domains. Gambit was used to create mesh files for use with Fluent. Gambit allows creating a combination of structured and unstructured meshes for both two-dimensional and three-dimensional geometries.

Procedure to create a 3D model of a smooth tube in Gambit:

a. Create an outline of the face using arcs and lines.

b. Create a face from the above sketched outline.

c. Extrude the face to the required length using the sweep command.

Procedure to create a 3D model of a finned tube in Gambit:

a. Create the outline of the face without the fins using arcs and lines.

b. Create the face from the above sketched outline.

c. Extrude the face to the required length using the sweep command.

d. Create an outline of the face of the fins using arcs and lines.

e. Create a face from the about outline and extrude it.

f. Join the fin and the fluid volume by connecting their respective faces and the vertices.

g. Define the zones and the boundary conditions for the smooth/finned tube.

The boundary conditions used for modeling the smooth/finned tube are discussed below.

a. *Velocity inlet* – It is used to define the velocity and other scalar properties like temperature of the flow at the inlet.

b. *Pressure outlet* – It is used to define the static pressure at flow outlets and other scalar variables like temperature in case of backflow in the tube.

c. *Symmetry* – It is used to define the planes of symmetry in the geometry.

d. *Wall* - It is used to define the fluid-solid interface. Once the boundary conditions are defined, then the continuum zones are defined for the different volumes in the geometry. The fin is defined to be a solid and region through which the PCM fluid flows is defined as a liquid.

Meshing the geometry:

a. Specify boundary layers at the surface of the wall.

b. Mesh the inlet face of the geometry. Refine the mesh near the corners of the

finned tube.

c. Repeat the same procedure for the outlet of the tube.
d. Mesh the length of the tube using the successive ratio option (a ratio value of 1.003 was used). This option increases the mesh count in the entrance region of the tube and decreases it gradually along the length of the tube.
e. Mesh the inlet face of the tube using the quad pave command which meshes the face using un-structured quadrilateral elements.
f. Use the cooper mesh scheme under the volume mesh commands to mesh the volume with 3-D hexahedron elements.
g. Check the aspect ratio and skewness of the geometry.
h. Export the mesh file.

3. Grid check and Scaling

Once the mesh is imported into FLUENT, the grid has to be checked for skewness and negative volume. If there are any negative volumes, the geometry has to be meshed again as it will cause the solution to diverge or yield incorrect results. Once this is done, the geometry can be scaled, if needed. Scaling is useful when the length of the geometry has to be increased when fully developed conditions are not reached for a length of the tube. This saves time as one does not need to create a new geometry and the corresponding mesh again.

4. Compiling UDF's

Fluent allows the user to initialize material properties, boundary conditions and post process results using a C program. This C program has to be compiled and built before it can be used by FLUENT. Before initializing the material properties, the user defined function is loaded through FLUENT and checked for errors. The UDF's are made available for use only if it is complied successfully.

5. Definition of the fluid and solid properties

Enter the appropriate values for the fluid and solid properties under the DEFINE-MATERIALS section. Enter the values of density, viscosity, conductivity and specific heat for the fluid and density, conductivity and specific heat for the solid continuum domain. The specific heat is defined as a function of local fluid temperature by using the piece-wise polynomial option. The liquid conductivity is set as a user defined function which is imported into FLUENT.

6. Definition of boundary conditions

The boundary conditions can be specified in Gambit and can also be reassigned in FLUENT. The fully developed velocity profile is given as the inlet condition along with an initial value of temperature. The wall is initialized with heat flux or a constant temperature depending on the nature of the problem. In some cases where a fully developed velocity and a temperature profile are required, the profiles are imported and initialized as inlet conditions.

APPENDIX C

Solver

1. Select segregated solver from DEFINE-MODELS-SOLVER menu.
2. Switch on the Energy Equation from DEFINE-ENERGY menu.
3. Select the Laminar option under the DEFINE-VISCOUS menu.
4. Set Under-relaxation factors (Pressure - 0.3, Density -1.0, Momentum - 0.7, Energy - 1.0)
5. Select Discretization Scheme (Pressure – Second Order, Momentum - Second Order Upwind, Pressure velocity Coupling - SIMPLE, Energy - Second Order Upwind)
6. Initialize the solution.
7. Set values of residuals for continuity, momentum and energy equations to 10^{-6}.
8. Iterate.

APPENDIX D

Post-processor

FLUENT provides some powerful visualization tools for interpreting results. Tools like x-y plots, contours, grid display aid in visualizing and exporting most flow properties like pressure, temperature, velocity to other software's like TECPLOT and EXCEL. Grid adaption can be done to accommodate large gradients in pressure and temperature. This option saves time spent on meshing the model again to account for the gradients by locally refining the meshes where the gradients are large. Fluent has options to create surfaces (points, lines, planes) on the geometry. For example it is possible to create iso-surfaces based on grid co-ordinates, planes on only the fluid zone without the plane intersecting the solid zone. Fluent can also compute surface integrals of flow properties on surfaces. Some of the options available are listed below.

a) Maximum, minimum, average values of properties on surface faces

b) Maximum, minimum, average values of properties on surface vertex

c) Mass flow weighted, area weighted average of flow properties

APPENDIX E

Modeling Parameters for Smooth Circular Tube

All the simulations pertaining to the smooth circular tube had the following parameters unless specified.

a. Tube diameter: 0.002m

b. Reynolds number: 485.0

c. Phase change material volumetric concentration: 15.0%

d. Melting range: 0.07

e. $Pe_f (r_p/r)^2 = 1$

f. Sub-cooling: 0.0

g. Conductance ratio: 4.0

h. Latent heat of phase change material: 230 kJ kg^{-1}

i. Boundary Condition: H1 and T boundary condition

j. Fully developed velocity at the inlet

Physical properties of the carrier fluid and phase change material

	Density kg m^{-3}	Specific Heat J kg^{-1} K^{-1}	Thermal Conductivity W m^{-1} K^{-1}	Kinematic Viscosity m^2 s^{-1}
Water	997	4180	0.606	9.07 x 10^{-7}
Microcapsule	946.4	1973.1	0.15	-

APPENDIX F

Modeling parameters for a Finned Tube

All the simulations pertaining to the smooth circular tube had the following parameters unless specified.

a. Tube diameter: 0.002 m
b. Fin angle: 6°
c. Fin conductivity: k_b (same as that of the bulk conductivity of the PCM fluid) or k_{Al} (thermal conductivity of Aluminum, 202.4 W m^{-1} K^{-1})
d. Reynolds number: 485.0
k. Pef $(r_p/r)^2 = 5$
e. Phase change material volumetric concentration: 15%
f. Melting range: 0.07
g. Sub-cooling: 0.0
h. Conductance ratio: 4.0
i. Latent heat of phase change material: 230 kJ kg^{-1}
j. Boundary Condition: H2 and T boundary condition
k. Fully developed velocity at the inlet
l. PCM liquid thermal conductivity = bulk conductivity of the PCM fluid

VITA

Name: Gurunarayana Ravi

Address: Texas A&M University,
Department of Mechanical Engineering,
3123 TAMU,
College Station, Texas 77843-3123

Email Address: guru25485@yahoo.com

Education: B.E., Mechanical Engineering, Anna University, India, 2006
M.S., Mechanical Engineering, Texas A&M University, 2008